AGU PUBLICATIONS

JGR

Journal of Geophysical Research: Planets

RESEARCH ARTICLE
10.1002/2015JE004972

Key Point:
- Carbonates coexist with phyllosilicates in exhumed Noachian rocks in several regions of Mars

Correspondence to:
J. J. Wray,
jwray@gatech.edu

Citation:
Wray, J. J., S. L. Murchie, J. L. Bishop, B. L. Ehlmann, R. E. Milliken, M. B. Wilhelm, K. D. Seelos, and M. Chojnacki (2016), Orbital evidence for more widespread carbonate-bearing rocks on Mars, *J. Geophys. Res. Planets*, *121*, 652–677, doi:10.1002/2015JE004972.

Received 9 NOV 2015
Accepted 3 APR 2016
Accepted article online 7 APR 2016
Published online 22 APR 2016

Orbital evidence for more widespread carbonate-bearing rocks on Mars

James J. Wray[1], Scott L. Murchie[2], Janice L. Bishop[3], Bethany L. Ehlmann[4], Ralph E. Milliken[5], Mary Beth Wilhelm[1], Kimberly D. Seelos[2], and Matthew Chojnacki[6]

[1]School of Earth and Atmospheric Sciences, Georgia Institute of Technology, Atlanta, Georgia, USA, [2]The Johns Hopkins University/Applied Physics Laboratory, Laurel, Maryland, USA, [3]SETI Institute, Mountain View, California, USA, [4]Division of Geological and Planetary Sciences, California Institute of Technology, Pasadena, California, USA, [5]Department of Geological Sciences, Brown University, Providence, Rhode Island, USA, [6]Lunar and Planetary Laboratory, University of Arizona, Tucson, Arizona, USA

Abstract Carbonates are key minerals for understanding ancient Martian environments because they are indicators of potentially habitable, neutral-to-alkaline water and may be an important reservoir for paleoatmospheric CO_2. Previous remote sensing studies have identified mostly Mg-rich carbonates, both in Martian dust and in a Late Noachian rock unit circumferential to the Isidis basin. Here we report evidence for older Fe- and/or Ca-rich carbonates exposed from the subsurface by impact craters and troughs. These carbonates are found in and around the Huygens basin northwest of Hellas, in western Noachis Terra between the Argyre basin and Valles Marineris, and in other isolated locations spread widely across the planet. In all cases they cooccur with or near phyllosilicates, and in Huygens basin specifically they occupy layered rocks exhumed from up to ~5 km depth. We discuss factors that might explain their observed regional distribution, arguments for why carbonates may be even more widespread in Noachian materials than presently appreciated and what could be gained by targeting these carbonates for further study with future orbital or landed missions to Mars.

1. Introduction

1.1. The Missing Martian Carbon

Modern Mars has a $<$10 mbar atmosphere dominated by CO_2. A thicker ancient atmosphere is suggested by estimates of outgassed volatiles and by isotopic and geomorphologic observations [e.g., *Pollack et al.*, 1987; *Jakosky and Phillips*, 2001]. Recent constraints from ~3.6 Ga geomorphological features have suggested an ancient atmosphere $>$100 mbar [*Manga et al.*, 2012] to $<$2 bar [*Kite et al.*, 2014], but these constraints likely apply to Late Noachian or younger rocks. The earlier Noachian conditions ($>$3.8 Ga) [*Werner and Tanaka*, 2011] could have been different; indeed, isotopic evidence suggests loss of ~50–90% of Mars' atmosphere within the first hundreds of Myr [*Jakosky and Jones*, 1997]. Nonthermal escape processes appear capable of removing only up to ~10 mbar [e.g., *Chassefière et al.*, 2013] or at most ~100 mbar CO_2 over the past 4.1 Gyr [*Lammer et al.*, 2013], so another sink for the early atmosphere is needed.

Ancient atmospheric CO_2 could also have been sequestered via dissolution in surface waters, yielding HCO_3^- and CO_3^{2-} ions that combined with cations weathered from silicate crustal material, forming carbonate minerals [e.g., *O'Connor*, 1968; *Goldspiel and Squyres*, 1991]. This mechanism, which should have left an imprint on the atmospheric CO_2 isotopes, is consistent with the modern average total atmospheric pressure near the H_2O triple point (i.e., the minimum H_2O partial pressure at which liquid H_2O is stable); further sequestration in surface water bodies would have been inhibited by the instability of such bodies against boiling [*Kahn*, 1985; *Richardson and Mischna*, 2005]. Pure water would evaporate rapidly under the low H_2O partial pressure of the modern atmosphere, but its stability is enhanced by salinity [*Ingersoll*, 1970] and/or in thermally favorable local environments [*Hecht*, 2002]. Carbonates can also form in thin H_2O films under the dry conditions of modern Mars [*Booth and Kieffer*, 1978; *Shaheen et al.*, 2010], but this process appears to be self-limiting and could likely store only a few tens of millibars CO_2 [*Stephens and Stevenson*, 1990; *Stephens et al.*, 1995] and also may require precursor minerals not known to exist widely on Mars, such as portlandite [*Garenne et al.*, 2013]. Hence, evidence for substantial carbonate formation would likely attest to at least locally wetter conditions in the Martian past.

1.2. Carbonates of Unknown Provenance

Carbonates were first identified tentatively in regional-to-global spectra acquired by ground-based, Earth-orbiting, and airborne telescopes [*Blaney and McCord*, 1989; *Pollack et al.*, 1990; *Lellouch et al.*, 2000] and by

the infrared spectrometers on Mariner 6 and 7 [*Calvin et al*., 1994]. Such spectra are dominated by atmospheric and/or surficial dust. Although these detections are now largely viewed as equivocal [e.g., *Calvin and Bell*, 2008], the hydrous Mg-carbonates inferred to match the observations of *Calvin et al*. [1994] are partially consistent with more recent detections [e.g., *Ehlmann et al*., 2008; *Palomba et al*., 2009]. The Thermal Emission Spectrometer (TES) aboard Mars Global Surveyor (MGS) showed evidence for minor carbonate (~2–5 weight %) in global Martian dust, likely at <10 μm grain sizes [*Bandfield et al*., 2003]. Mg-carbonate was later also inferred in situ as a minor regolith component using Mini-TES on the Mars Exploration Rovers [*Christensen et al*., 2004]. Independent evidence for minor carbonate in the regolith came from the Thermal and Evolved Gas Analyzer on the Phoenix polar lander, which landed at 68°N and measured a high-temperature CO_2 release consistent with breakdown of a Ca-rich carbonate at 3–6% in the soils [*Boynton et al*., 2009; *Sutter et al*., 2012]. Phoenix Wet Chemistry Lab data support this interpretation [*Kounaves et al*., 2010a, 2010b], and a separate Fe/Mg-rich carbonate decomposing at lower temperature (~1 wt % abundance) may explain a distinct lower temperature CO_2 release [*Sutter et al*., 2012], although there are other possible causes [*Cannon et al*., 2012]. These Ca-rich carbonates could either have formed in situ from atmospheric CO_2 or via cation replacement of dust-deposited Mg-carbonates, or they could be derived from a regional rock unit [*Boynton et al*., 2009; *Sutter et al*., 2012]. The Mars Science Laboratory rover Curiosity's evolved gas analyses have also shown CO_2 releases consistent with less than ~1–2% Fe/Mg-rich carbonates in the <150 μm size fraction of soil in Gale crater [*Leshin et al*., 2013; *Archer et al*., 2014] and possibly at $<1\%$ abundance in the ancient sedimentary rocks of Yellowknife Bay [*Ming et al*., 2014]. However, the low temperatures at which CO_2 evolved from these samples may also be consistent with a noncarbonate source such as oxalate minerals [*Eigenbrode et al*., 2014; *Niles et al*., 2015; *Applin et al*., 2015], predicted by *Benner et al*. [2000] to be a stable end product of oxidizing meteoritic organics at the Martian surface.

Carbonates have been found in meteorites from Mars, including the nakhlites and ALH84001 [e.g., *Mittlefehldt*, 1994; *Bridges and Grady*, 2000]; carbonates in chassignites and in the shergottite EETA79001 have less clear-cut isotopic or stratigraphic evidence for a Martian origin [*Gooding et al*., 1988; *Wentworth and Gooding*, 1994; *Beck et al*., 2006]. ALH84001 is the oldest of these, at ~4.1 Ga with ~3.9 Ga carbonates [*Lapen et al*., 2010; *Borg et al*., 1999]; many of its carbonates occur in submillimeter concretions that exhibit chemical zonation from Ca,Fe-rich cores to Mg-rich rims. Their nonequilibrium compositions and stable isotope variations suggest a dynamic, short-lived aqueous environment for carbonate formation at relatively low temperature [e.g., *Valley et al*., 1997], although hydrothermal mechanisms have also been proposed [*Harvey and McSween*, 1996]. Recent clumped isotopic studies of ALH84001 carbonates suggest that they formed not in a lake open to the atmosphere but in a shallow subsurface water body (meters to decameters deep) at mild temperatures of 18 ± 4°C [*Halevy et al*., 2011], in which declining CO_2 partial pressure within the aquifer led to the observed chemical zonation [*Van Berk et al*., 2011]. Similar formation depths have been inferred for the veined carbonates and phyllosilicates in the nakhlites [*Changela and Bridges*, 2011]. In both cases, triple oxygen isotope analyses of the carbonates indicate disequilibrium relative to Mars' silicate crust [*Farquhar et al*., 1998; *Farquhar and Thiemens*, 2000]. Their ^{13}C enrichments suggest that the contemporaneous atmosphere had already undergone substantial loss to space [e.g., *Niles et al*., 2010], although additional post-Noachian loss is implied by comparing ALH84001 carbonates to the modern atmosphere [*Shaheen et al*., 2015]. While informative, these carbonates constitute only up to ~1% by volume abundance of their meteoritic host materials [*Bridges et al*., 2001].

1.3. Carbonates in Outcrop

Several searches via spectroscopy from Mars orbit revealed no carbonate-bearing rocks on Mars (to upper limits of ~10–15% abundance) at scales of greater than a few kilometers, as observed in both thermal emission with TES and near-IR reflectance with Mars Express OMEGA or Phobos 2's Imaging Spectrometer for Mars [e.g., *Murchie et al*., 2000; *Christensen et al*., 2001; *Bibring et al*., 2006]. *Jouglet et al*. [2007] conducted a comprehensive global search for carbonates using OMEGA data, focusing on one of the strongest spectral features for anhydrous carbonates, at ~3.4 μm. The negative results of these searches were surprising after decades of speculation about a global equivalent layer tens of meters thick [e.g., *Toon et al*., 1980; *Kahn*, 1985; *Warren*, 1987] and/or local accumulations in sedimentary basins [*McKay and Nedell*, 1988; *Forsythe and Zimbelman*, 1995]. Thermal infrared studies of several candidate basins revealed no abundant carbonates [*Ruff et al*., 2001; *Stockstill et al*., 2005, 2007], and the Spirit rover's landing site in Gusev crater—a likely former lake basin—was found to be covered in basaltic lavas rather than carbonate-rich sediments [*Squyres et al*., 2004].

Several explanations were proposed for the initial failure to discover widespread carbonate-rich bedrock. It was suggested that perhaps Mars was simply too cold and dry for carbonate formation over the vast majority of its history [*Christensen et al*., 2001], but subsequent detections of widespread aqueous mineral deposits [*Poulet et al*., 2005; *Bibring et al*., 2006; *Mustard et al*., 2008; *Murchie et al*., 2009a] imply that another explanation is needed for the scarcity of carbonates. *Ehlmann et al*. [2011] suggested that most clays formed through isochemical alteration in the subsurface, largely out of contact with the CO_2-rich atmosphere and thus under conditions favoring oxide and secondary silicate formation over carbonates. The occurrence of sulfates suggested to some researchers that lakes and seas on the surface of early Mars were too acidic for carbonate formation [*Fairén et al*., 2004; *Bullock and Moore*, 2007]. *Bibring et al*. [2006] suggested that even if early conditions were conducive to forming carbonates, they have since been eliminated by weathering under more acidic conditions. One possible fate of calcium carbonates weathered under such acidic conditions is formation of bassanite ($CaSO_4 \cdot ½H_2O$) [*Vaniman et al*., 2008], which has indeed been found at the base of the ancient clay-rich Mawrth Vallis layered phyllosilicate-rich deposit [*Wray et al*., 2010]. The fate of any carbon liberated by weathering of putative massive deposits is unclear, although one possibility is reprecipitation at greater depths where fluids became neutralized through interaction with the basaltic crust [*Fernández-Remolar et al*., 2011]. Alternatively, experimental and analog studies suggest mere surficial weathering of carbonates (formation of a sulfate coating) [*Clark et al*., 1979; *Cloutis et al*., 2010], which could mask their spectral signature and thus would avoid the "missing carbon" problem. However, such surficial processes would not have prevented formation and preservation of carbonate at depth [*Chassefière and Leblanc*, 2011]. Based on thermodynamic arguments and the apparent absence of carbonates in most Martian clay-bearing deposits, *Chevrier et al*. [2007] argued for a persistently low atmospheric pCO_2 even early in Mars history. *Orofino et al*. [2009] argued on geochemical grounds that carbonates would constitute at most a few percent of paleolake sediment volumes, possibly below the limits of detection via remote sensing.

Using higher spatial resolution reflectance spectroscopy, Mg-rich carbonate has been identified in bedrock outcrops adjacent to the Isidis basin [*Ehlmann et al*., 2008; *Brown et al*., 2010; *Bishop et al*., 2013a]. Mg-carbonate has also been confirmed in situ by Spirit in Gusev crater, where the Comanche outcrop hosts 16–34 wt % carbonate as estimated by three complementary chemical and mineralogical data sets [*Morris et al*., 2010b]. Mg-carbonate in nearby outcrops has also been reported from orbit [*Carter and Poulet*, 2012]. The preservation of substantial olivine in these carbonate-rich rocks was interpreted to implicate hydrothermal alteration at relatively low water activity [*Morris et al*., 2010b], but a lacustrine evaporative origin has also been proposed [*Ruff et al*., 2014], and geochemical modeling indeed favors low-temperature (<85°C) formation from an environment (lake or aquifer) open to CO_2 exchange with a ~0.5–2 bar Late Noachian atmosphere over at least ~10^5 years [*Van Berk et al*., 2012].

Fe/Ca-carbonates, expected to precipitate from Martian brines at higher water activity [e.g., *Catling*, 1999], have been reported in the $D \sim 65$ km Leighton crater on the western flank of Syrtis Major [*Michalski and Niles*, 2010]. Here carbonate is associated with phyllosilicates in layered deposits exposed in Leighton's central uplift from an estimated depth of ~6 km. Ca/Fe-carbonates have also been reported in two crater central uplifts in Terra Tyrrhena [*Carrozzo et al*., 2013], in the walls of a crater into Noachian materials in the Eridania basin [*Gilmore et al*., 2014; *Korn and Gilmore*, 2015], in Capri Chasma at the eastern end of Valles Marineris [*Jain and Chauhan*, 2015], and on the floor of Robert Sharp crater just west of Gale crater [*Carter et al*., 2015]. However, it is unclear to what extent these isolated carbonate detections reflect widespread aqueous paleoenvironments or, alternatively, only localized alkaline conditions. Most of these Fe/Ca-carbonate detections from orbit occur in materials exposed—by impact or tectonics—from depth.

Here we describe new orbital evidence for regional occurrences of formerly buried, ancient Fe- and/or Ca-rich carbonate-bearing rocks, which provide new insights into what conditions may have allowed formation and preservation of Martian carbonates. In particular, we evaluate the updated global distribution of carbonate-bearing rocks relative to major regional features such as giant impact basins and anomalous chemical provinces. We explain how additional near-surface carbonates might have escaped detection thus far and discuss the implications of these carbonates for the planet's environmental history.

2. Methodology

Carbonates exhibit diagnostic spectral features due to vibrational energy level transitions of the CO_3^{2-} ion. The fundamental modes active in carbonates correspond to wavelengths of ~7, ~11.5, and ~14 μm [e.g.,

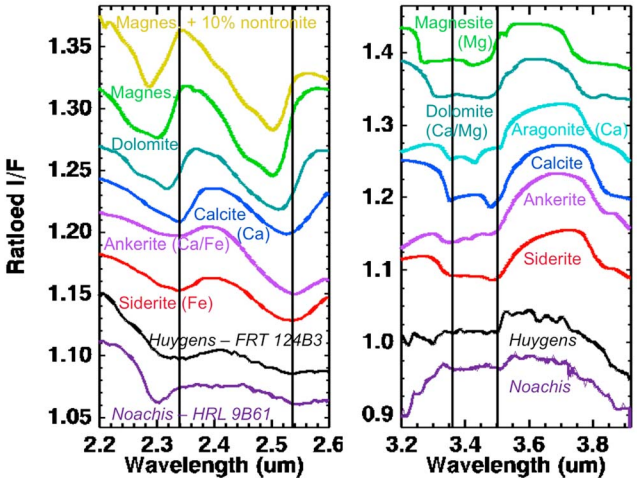

Figure 1. CRISM spectra (bottom) compared to rescaled carbonates from the CRISM and USGS spectral libraries [*Murchie et al.*, 2007; *Clark et al.*, 2007]. Dolomite ($CaMg(CO_3)_2$) is sample HS102.3B, aragonite ($CaCO_3$) is LACB02A, calcite ($CaCO_3$) KACB10A, ankerite ($CaFe(CO_3)_2$) LACB01A, and siderite ($FeCO_3$) is CAGR03. Magnesite ($MgCO_3$) and its mixture with nontronite are from *Bishop et al.* [2013b]. Laboratory spectra have been rescaled for ease of comparison. Vertical lines are at 2.34, 2.54, 3.36, and 3.5 μm.

Huang and Kerr, 1960; *Adler and Kerr*, 1962]. Strong overtone and combination bands appear at ~3.4–3.5 and ~3.9 μm (Figure 1, right), although in hydrous carbonates these can be masked by the strong H_2O-related features around 3 μm [*Miyamoto and Kato*, 1990; *Cloutis et al.*, 2000; *Harner and Gilmore*, 2015; *Applin et al.*, 2014]. Higher-order overtones and combination bands occur in the shortwave infrared, most notably at 2.3–2.35 and 2.5–2.55 μm [e.g., *Hunt and Salisbury*, 1971]. These bands are intrinsically weaker and, for example, were not detected in the ALH 84001 spectral analyses that identified minor carbonates in the mid-IR region [*Bishop et al.*, 1998a, 1998b]. But, as with the fundamental bands at longer wavelengths [*Adler and Kerr*, 1963], the shapes and central wavelengths of the ~2.3 and ~2.5 μm absorptions can be diagnostic of the carbonate cation(s) [*Gaffey*, 1987], polymorph [*Gaffey*, 1986], and hydration state [*Smyth et al.*, 2014] (Figure 1, left).

We identify carbonates using the Mars Reconnaissance Orbiter's Compact Reconnaissance Imaging Spectrometer for Mars (CRISM), which samples the ~0.4–3.9 μm spectral range at 6.55 nm/channel [*Murchie et al.*, 2007]. Standard atmospheric and photometric corrections were applied to filtered CRISM I/F data [*Murchie et al.*, 2009b], including the "volcano-scan" method of CO_2 removal [e.g., *McGuire et al.*, 2009]. Spectra of interest were ratioed to bland areas in the same scene—in the same detector column, where feasible—to mitigate systematic artifacts. Early CRISM-based studies of Martian carbonates suffered from noise in the 3–4 μm region and an artifact at 3.18 μm that could obscure the 3.4 μm carbonate absorption and calcite-specific absorptions at 3.1–3.2 μm [*Murchie et al.*, 2009b]. Fortunately, these issues have been moderated in "version 3" of the CRISM calibration available for all data products since 2011, enabling utilization of CRISM's full spectral range for carbonate identification. We do so with the caveats that we make no attempt to model and remove the thermal emission that competes with surface reflectance at the longest wavelengths and that many observations still show spectral structure in the 3–4 μm range that we do not fully understand. To minimize "false positive" carbonate detections, we consider consistency with laboratory carbonates at these wavelengths to be necessary but not sufficient for identification.

Minor artifacts remaining in the spectra include unusable data at ~2.7 μm due to a saturated atmospheric CO_2 absorption there, and intermittent spikes at the ~1.65 μm wavelength of a detector filter boundary [*Murchie et al.*, 2007]. CRISM pixels having spectral absorptions characteristic of particular minerals can be mapped using spectral summary parameters [e.g., *Pelkey et al.*, 2007; *Viviano-Beck et al.*, 2014]. These mineral indicators, such as absorption band depths, reflect a combination of mineral abundance within a pixel as well as textural effects such as grain size. Key summary parameters for mapping carbonates include BD2500 for mapping the 2.5 μm absorption [*Ehlmann et al.*, 2009], D2300 for the 2.3 μm absorption, BDCARB for the pair of bands at ~2.33 and ~2.53 μm, and CINDEX for the 3.9 μm absorption [*Pelkey et al.*, 2007]. The 3.9 μm band depth is considered as evidence for carbonates only in scenes where it appears spatially correlated with the 2.3 and 2.5 μm band depths.

Nonlinear spectral mixture modeling to estimate the abundances of carbonate minerals is ongoing [e.g., *Wiseman et al.*, 2014; *Edwards and Ehlmann*, 2015] but is an intensive process not included as part of our present study. Mixture modeling for rocks can be more straightforward at thermal infrared wavelengths, where single scattering dominates and spectra add nearly linearly [*Ramsey and Christensen*, 1998; *Feely and*

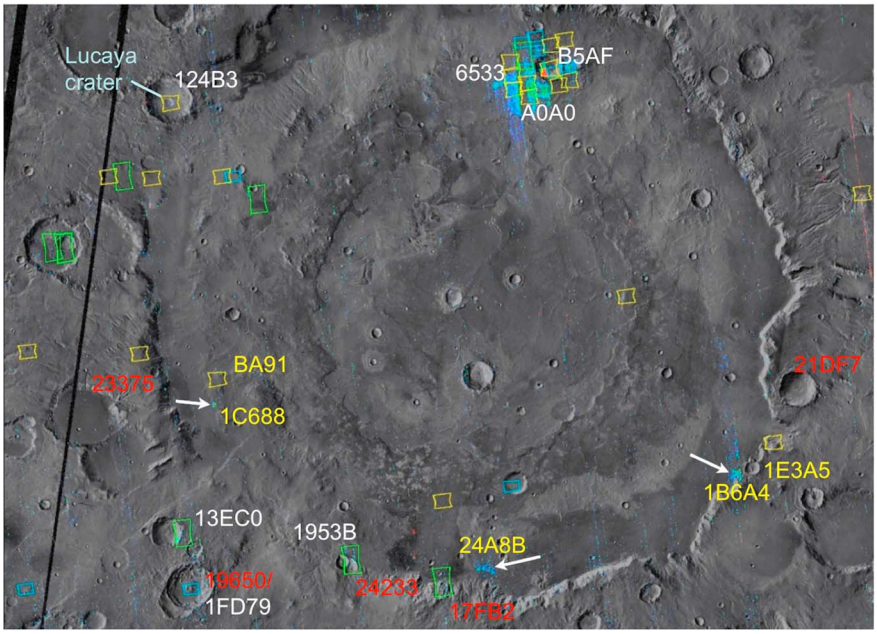

Figure 2. Carbonates and clay minerals in and around Huygens basin (D ~ 467 km). THEMIS daytime IR mosaic (gray scale) overlain by CRISM multispectral map of the 2.3 μm band strength on a color scale (blue➔red), with targeted hyperspectral image footprints outlined (yellow = FRT, green = HRL, and blue = HRS) or, for more recent images of interest, indicated by arrows. CRISM hyperspectral images examined are labeled with hexadecimal IDs in white (confirmed carbonate), yellow (possible detection), or red (nondetection having significance for understanding the regional distribution). In this and subsequent figures (unless otherwise indicated), north is up.

Christensen, 1999]. The coarser resolution of TES and Mars Odyssey's Thermal Emission Imaging System (THEMIS) relative to CRISM, plus textural effects such as high porosity [*Kirkland et al*., 2003], make definitive identification challenging for small deposits, but possible for the largest known deposits where exposures are at kilometer scales [*Edwards and Ehlmann*, 2015]. We focus here on using CRISM to determine the presence or absence of carbonate, with geologic context provided by visible-wavelength images from the High Resolution Imaging Science Experiment (HiRISE) and Context Camera (CTX) on MRO, and the Mars Orbiter Laser Altimeter (MOLA) on MGS.

3. Huygens Basin Region

3.1. Spectral Analysis

The ~450 km diameter (D) Huygens basin (~14°S, 55°E) northwest of Hellas exposes ancient Noachian materials of diverse compositions [*Seelos et al*., 2010; *Ackiss et al*., 2013]. In and around the basin, CRISM spectra of several outcrops—most exposed by craters superposed on the basin rim (Figure 2)—exhibit a distinct spectral phase with broad absorptions consistently centered at 2.33 and 2.53 μm, similar in position to vibrational bands in carbonates such as siderite (Figures 1 and 3). These outcrops also share a broad spectral curvature from 1 to ~1.8 μm in CRISM data, consistent with Fe-bearing carbonate, chlorite, or other ferrous phases [e.g., *Bishop et al*., 2013c], or possibly dehydrated Fe^{3+}-smectite [*Morris et al*., 2010a]. An assemblage containing chlorite is further implied by an additional weak feature at 2.25 μm in the CRISM spectrum in Figure 3. CRISM spectra of adjacent outcrops appear dominated by hydrated Mg-phyllosilicates (possibly smectites), and these also cooccur in the carbonate outcrops, producing the water-related absorptions at 1.40 and 1.91 μm and contributing to the depth and width of the 2.3 μm band (Figure 3). Additionally, the low continuum I/F values at ~3.2–3.3 μm in the CRISM spectra of Figure 1 (relative to pure carbonates) are due to stronger 3 μm H_2O absorptions in the carbonate-bearing materials than in the surroundings.

Several hydroxylated, noncarbonate minerals also absorb near 2.3 and/or 2.5 μm (Figure 3), but no linear mixture of these phases in our spectral libraries (e.g., chlorite + analcime) matches the CRISM absorptions as closely in position and shape as do Fe/Ca-carbonates (Figure 3). Additional absorptions at 3.5 and 3.9 μm provide

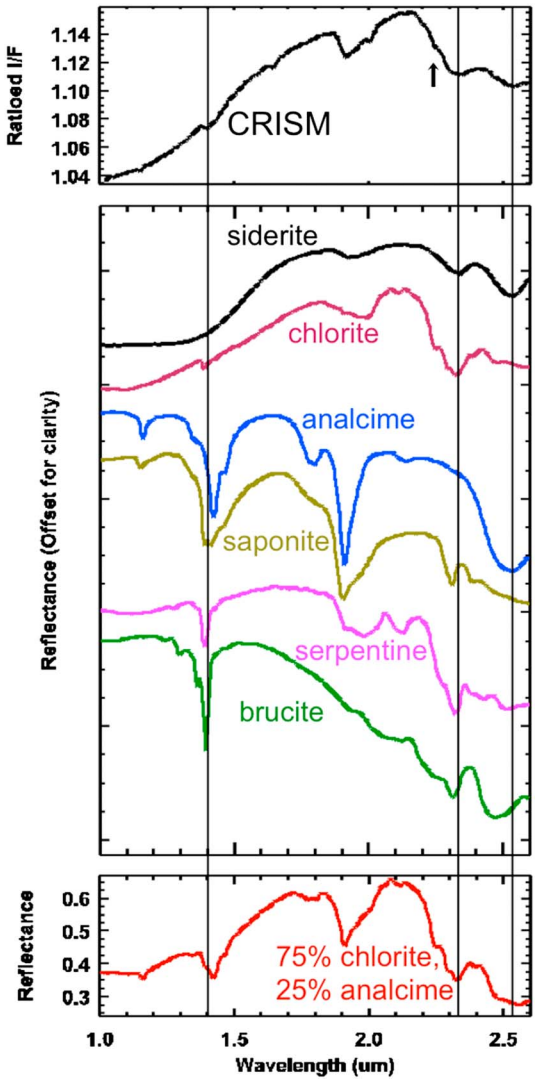

Figure 3. Spectrum from Huygens basin (CRISM FRT000124B3; 578 pixels averaged from area in Figure 5c) compared to minerals from the CRISM and USGS spectral libraries [*Murchie et al.*, 2007; *Clark et al.*, 2007]. Siderite is sample HS271.3B, chlorite is SMR-13.a, analcime GDS1, saponite SapCa-1, lizardite NMNHR4687.a, brucite HS247.3B. Carbonate (e.g., siderite or calcite/ankerite) reproduces the 2.33 and 2.53 μm bands better than any other mineral. The 1.4, 1.9 μm bands in the CRISM data, a subtle feature at 2.25 μm (arrow), along with a 2.3 μm absorption band depth greater than the 2.5 μm absorption band depth indicate the presence of Fe/Mg-phyllosilicate (smectite and/or chlorite) intermixed with carbonate. However, no linear mixture that excludes carbonate (e.g., chlorite + analcime, bottom panel) matches the CRISM data as well as mixtures that include carbonate. Vertical lines are at 1.4, 2.33, and 2.53 μm.

further evidence for Fe/Ca-carbonates (Figure 1). By contrast, in Mg-rich carbonates (magnesite or even dolomite) all these spectral features occur at distinctly shorter wavelengths. Aragonite has a more complex spectral structure at ~3.4 μm that we do not observe in the Huygens data, but other Ca/Fe-carbonates (calcite, ankerite, and siderite) appear equally consistent with the vibrational bands detected by CRISM [see also *Bishop et al.*, 2015].

Figure 2 shows the spatial distribution of carbonate detections across the basin. Here a "detection" requires observation of comparably strong and broad absorptions at ~2.33 and ~2.53 μm, a clear 3.9 μm absorption, and at least weak features consistent with carbonate spectra at 3.4–3.5 μm. "Possible detections" labeled in Figure 2 lack one of these features but exhibit the others, while absence of at least two such characteristics is grounds for labeling as a "non-detection." Even the full detections still typically show evidence for contributions from associated noncarbonate phases; as on the Huygens rim (Figure 3), the most widespread exposure on the basin floor (Figure 4) exhibits 1.4 and 1.9 μm bands of hydrous minerals and a complex structure in the 2.2–2.6 μm range, suggesting mixture with phyllosilicates.

3.2. Geologic Setting and Morphology

The most diagnostic carbonate signature found to date at Huygens basin (Figure 3) is in Lucaya crater (Figure 5), a $D \sim 34$ km central (floor) pit crater superposed on Huygens' rim crest (11.6°S, 52°E). Here carbonate and phyllosilicate-bearing materials can be mapped to specific outcrops on the central pit wall (Figure 5c); the strongest signatures are seen on the southeastern side, but smaller carbonate outcrops occur across the pit's ~6 km width (e.g., bright outcrops on the northern wall at 11.545°S, 51.922°E). The carbonate-bearing rocks are jointed and possibly layered (Figure 6a) and in some places are criss-crossed by protruding ridges (Figure 6b) that could be dikes or large mineralized veins. These characteristics are reminiscent of the carbonate (and phyllosilicate)-bearing outcrops in the central uplift of Leighton crater, ~600 km north/northeast of Lucaya [*Michalski and Niles*, 2010]. The detailed spatial distribution of mineral signatures (Figure 5c) suggests that the phyllosilicate signatures are concentrated in the ridged areas, which could indicate that they represent a later stage of alteration.

Huygens basin carbonates are observed most commonly in the ejecta and interiors of $D \sim 10$–40 km impact craters. Several of these craters, such as Lucaya and the unnamed crater in Figure 4, contain central pits. Lucaya's central pit is a floor pit; i.e., it does not sit atop a substantial summit and is significantly deeper than

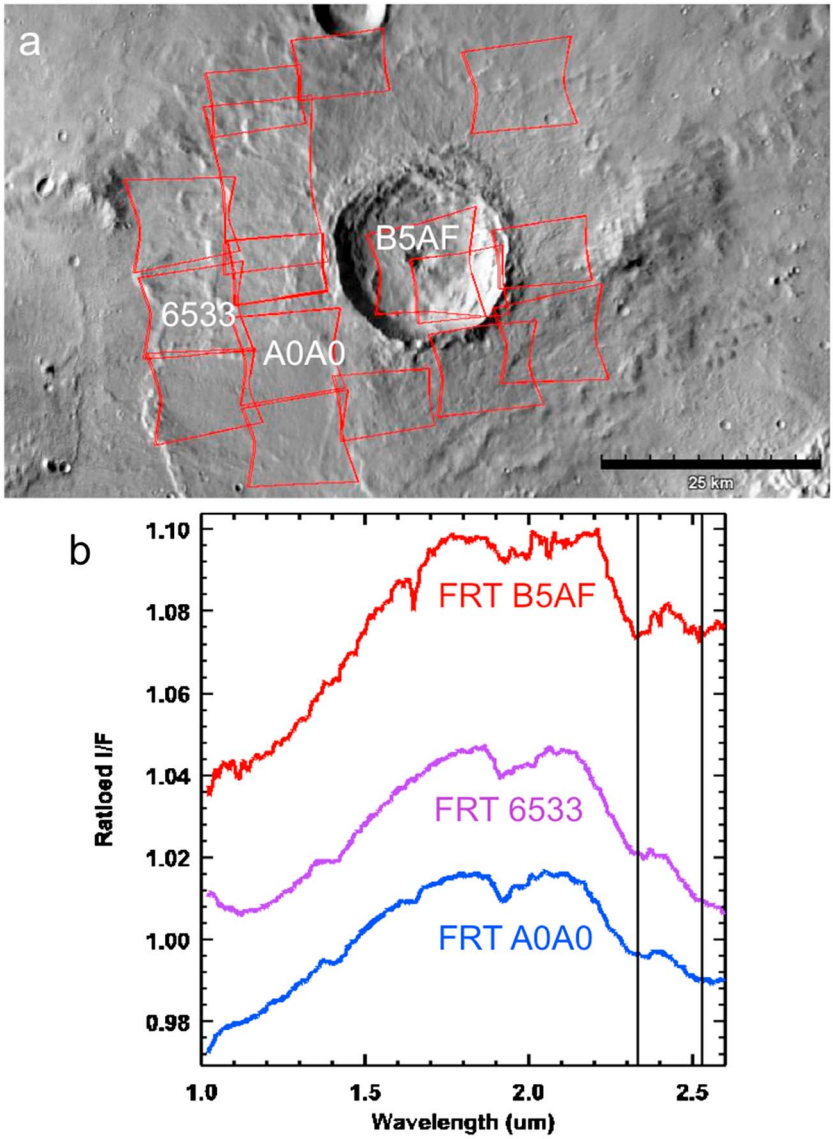

Figure 4. (a) Central pit crater on Huygens floor (11.2°S, 56.6°E). Most CRISM observations outlined contain secondary phases, ranging from carbonate to kaolinite, smectites, chlorite and prehnite (S. E. Ackiss et al., manuscript in preparation, 2015). (b) Spectra from the crater's central pit (top) and ejecta (middle, bottom) show similar characteristics to each other and to the CRISM spectrum in Figure 3. Vertical lines are at 2.33 and 2.53 μm.

the surrounding crater floor (Figure 5b). Crater floor pits throughout the solar system are thought to form from impacts into volatile-rich targets, generating impact melt that later drains into subsurface fractures, while its most volatile components are lost via vaporization [e.g., *Alzate and Barlow*, 2011; *Bray et al*., 2012; *Tornabene et al*., 2012]. An explosive component of volatile release from Lucaya's central pit is bolstered by its radial trend of decreasing thermal inertia from the crater center (Figure 5d), similar to numerous other Martian pit craters [*Williams et al*., 2015]. Release of CO_2 [e.g., *Hörz et al*., 2015] and H_2O from carbonate- and phyllosilicate-rich target rocks may have formed Lucaya's central pit, and the valleys emptying into it (Figure 5) could perhaps have been carved by impact-mobilized fluids; such valleys in central pit craters are otherwise relatively rare at the ice-poor equatorial latitudes of Mars [*Peel and Fassett*, 2013]. Lucaya's valleys are filled with younger aeolian bed forms (Figure 6a), which appear to be inactive, as several small impact craters are superposed on them. Indurated cross strata are visible among these bed forms, suggesting that later fluids may have dissolved some carbonates and reprecipitated them as sand cements [*Bourke and Wray*, 2011].

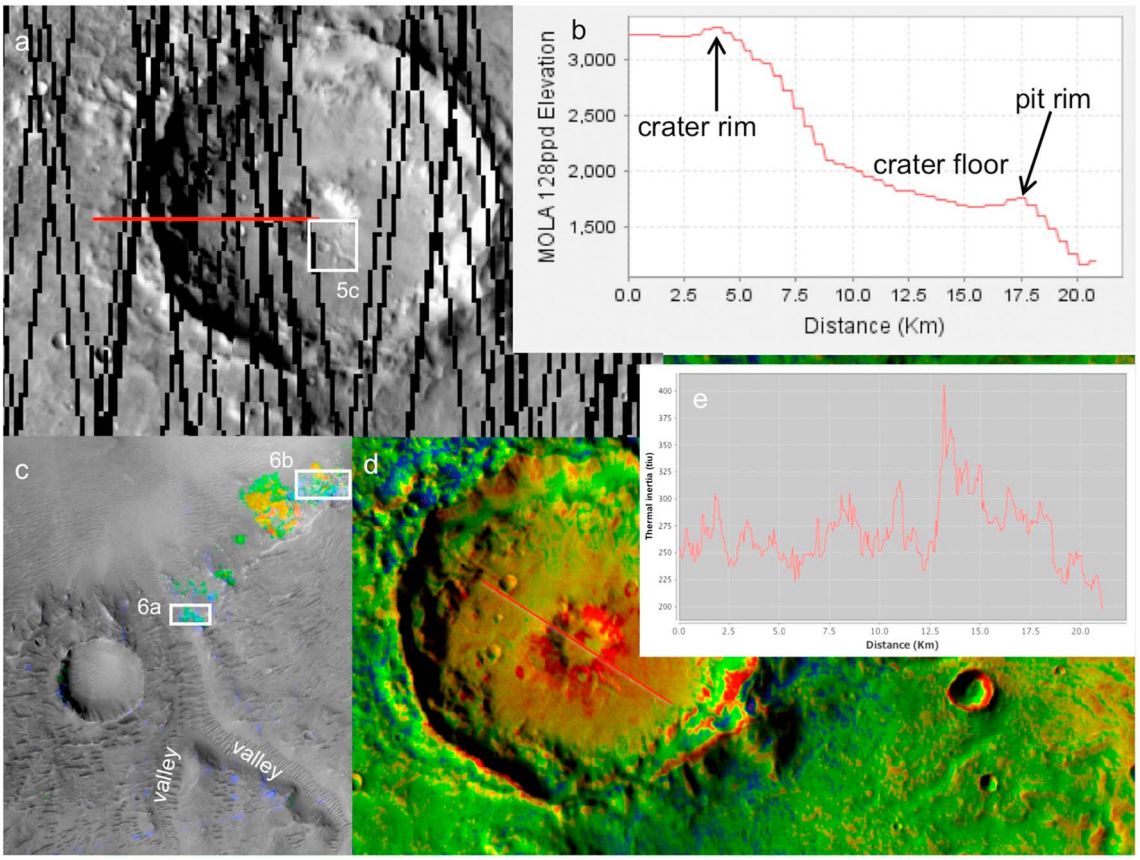

Figure 5. (a) $D \sim 34$ km crater Lucaya superposed on Huygens basin rim crest. MOLA laser shot ground tracks (black) displayed on THEMIS daytime IR mosaic, showing dense coverage. Red line marks the transect profiled from the MOLA digital elevation model in (b) cross section of western Lucaya, a floor pit crater. (c) CRISM FRT000124B3 overlain on HiRISE ESP_012897_1685_RED, highlighting phyllosilicate (orange) and carbonate (blue/green). R/G/B are the parameters D2300/BDCARB/CINDEX from *Pelkey et al.* [2007]. (d) THEMIS nighttime IR colorizing daytime IR mosaic of Lucaya crater and surroundings. Red line marks the transect profiled in (e) thermal inertia derived from THEMIS data [*Fergason et al.*, 2006; *Christensen et al.*, 2013], in units of $J \cdot m^{-2} s^{-0.5} K^{-1}$ (abbreviated "tiu," after *Putzig and Mellon* [2007]). Note peak value at the location of carbonate outcrops on the southeastern central pit wall.

The carbonate-bearing rocks in Lucaya's central pit today lie at a MOLA elevation of ~1.4–1.5 km relative datum [*Smith et al.*, 1999]. This is ~1.8 km below the pre-Lucaya local Huygens rim crest (Figure 5b); furthermore, up to ~3.3 km of structural uplift is predicted for central peak materials exposed by a crater of Lucaya's size [e.g., *Tornabene et al.*, 2008, equation (3)]. Therefore, prior to the impact that formed Lucaya crater, its carbonates may have been buried ~5 km beneath the Martian surface. Other confirmed carbonate detections on Huygens' rim or its proximal ejecta appear excavated from comparable depths, but not all deep rim exposures reveal unambiguous carbonates; e.g., FRT00021DF7 covers a $D \sim 25$ km central pit crater on Huygens' eastern rim exposing phyllosilicates, but no carbonates (Figure 2). However, spatial resolution can be critical to carbonate detection. For example, a $D \sim 32$ km crater on Huygens' southwest flank (Figure 7a) showed chlorite but no clear carbonates in its central uplift at ~36 m/pixel (CRISM HRS00019650), whereas at ~18 m/pixel (FRT0001FD79) carbonates are resolved (Figure 7b), likely originating from a depth similar to those in Lucaya. An adjacent $D \sim 21$ km crater's eastern wall was previously mapped as "clay-bearing" based on CRISM multispectral data at ~200 m/pixel (lower left corner of Figure DR1A of *Wray et al.* [2009]), but subsequent ~36 m/pixel hyperspectral data analysis confirms the presence of carbonates (HRL00013EC0) even relatively high on the crater wall. Here the preimpact depth of these materials can be no greater than a few hundred meters, indicating that carbonates may occur at varying depths across the region.

Carbonates are also found within Huygens basin as well as on its rim. Huygens has an uplifted central peak ring; carbonates on the basin floor all occur outside this ring, mostly adjacent to the dissected basin walls, and could have been eroded and transported from the basin rim. They occur from the north end of the basin to the south,

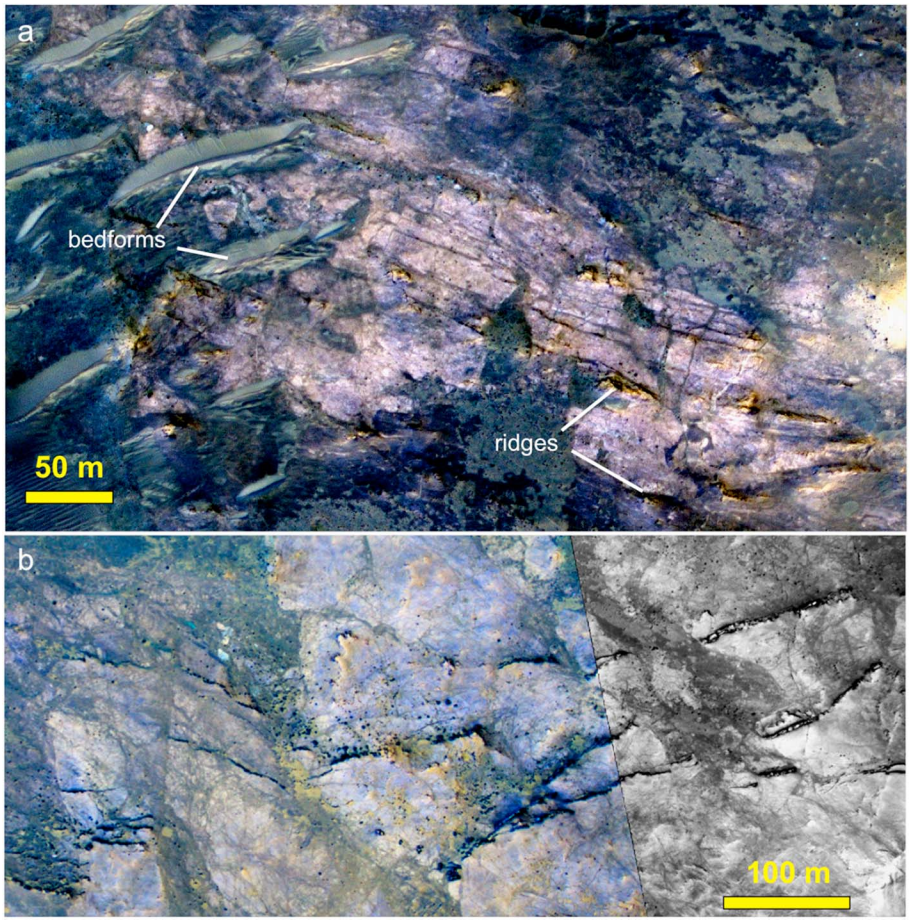

Figure 6. (a) Fractures and possible layers in carbonate-bearing rocks near mouth of the channel emptying into Lucaya crater's central pit (HiRISE ESP_012897_1685_IRB). (b) Large carbonate outcrop in the central pit of Lucaya crater. Color data are from HiRISE ESP_023024_1685_IRB, gray scale from ESP_013319_1685_RED. See Figure 5c for context.

exposed by craters (Figure 4) [see also *Wray et al.*, 2009, Figure DR1C] or, in one case, at the eroding edge of a dendritic (fluvial?) feature downslope from the basin wall-incising valleys (Figure 8).

Other carbonates lie beyond the probable original extent of Huygens' continuous ejecta. *Ehlmann et al.* [2008] reported a small exposure of carbonate-bearing rocks roughly 1200 km to the east/northeast in Terra Tyrrhena, in the central uplift of a $D \sim 35$ km crater at 5.63°S, 78.69°E (CRISM HRL000067B5). Within 300 km from this location, we report two additional crater exposures of carbonate (CRISM FRTs 64A8 and 79D1) (Figure 9). Spectra here suggest that these carbonates cooccur with phyllosilicates, and although all exhibit the four key absorptions listed in section 3.1 (e.g., Figure 7b), variation in the band positions makes it ambiguous whether these are Fe/Ca-carbonates akin to those in the Huygens region, or more Mg-rich carbonates as found ~600 km farther northeast in Libya Montes [*Bishop et al.*, 2013a], or a combination of both. Additional possible carbonate detections have been reported even farther east in Terra Tyrrhena [*Bultel et al.*, 2015b]. In the other direction, we find carbonates as far as 700 km southwest of Huygens, exposed in the walls of a cluster of eroded Noachian impact craters each ~40 km in diameter [*Irwin et al.*, 2012]. There they also cooccur with chlorite and Fe/Mg/Al-smectites, but at these locations (CRISM observations FRT00009318, HRL00013311) the carbonates themselves have absorptions centered at shorter wavelengths of ~2.31 and ~2.51 μm, indicating a more Mg-rich composition (R. P. Irwin III et al., manuscript in preparation, 2015). Thus, these newly reported carbonates span ~2300 km of highland terrain in this region (Figure 9); however, it is unknown whether all of these are genetically related or even coeval.

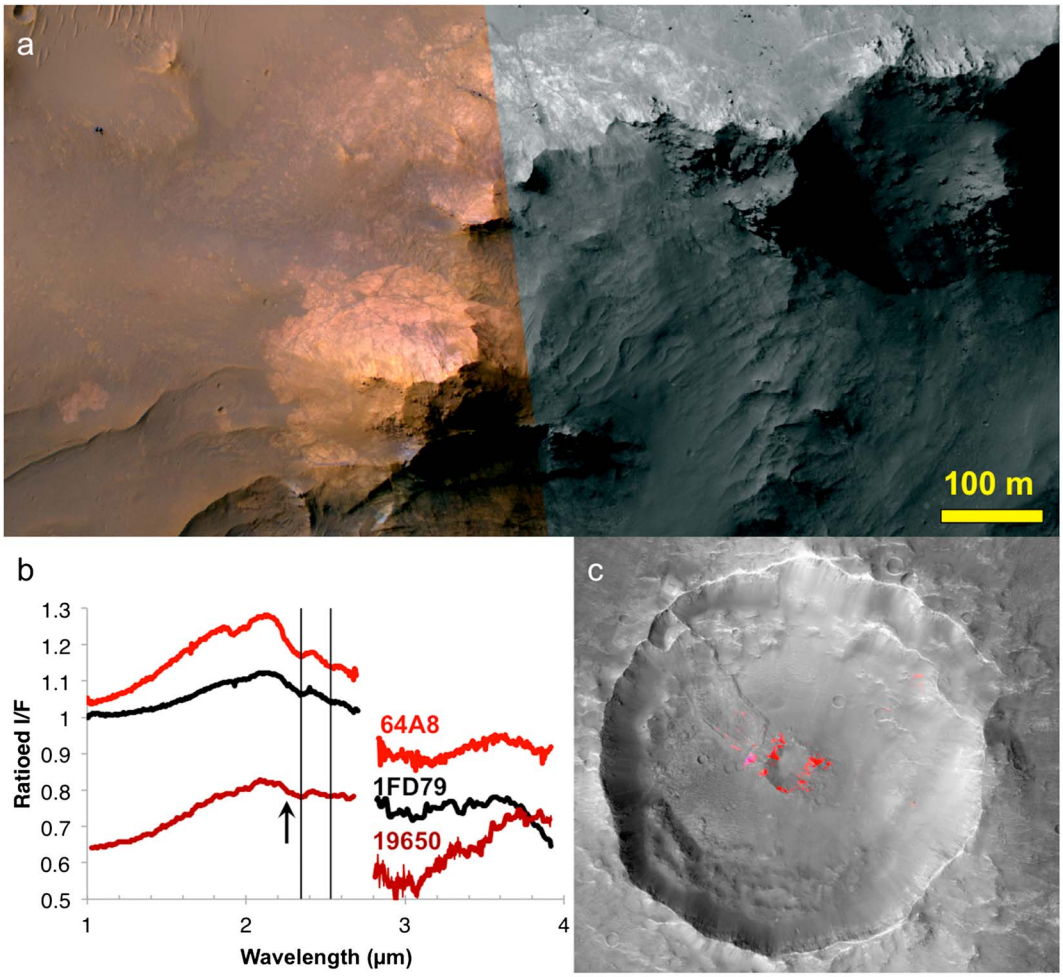

Figure 7. (a) Relatively light-toned phyllosilicate- and Fe/Ca-carbonate-bearing outcrops in central uplift of a $D \sim 32$ km crater (17.6°S, 52.2°E), where carbonates are detected in CRISM FRT0001FD79 (see lower left of Figure 2 for location). Note heterogeneity in outcrop color, albedo, and texture at the decameter scale of CRISM pixels (data are from HiRISE ESP_018277_1620). (b) At ~36 m/pixel (HRS 19650), after averaging enough pixels to mitigate noise, the outcrop in Figure 7 a has a spectrum resembling chlorite, with a strong 3 μm H_2O band, weaker ~2.5 than ~2.3 μm feature, and clear shoulder at 2.25 μm (arrow). At ~18 m/pixel, FRT 1FD79 resolves carbonate-rich subunits with stronger 2.5, 3.35/3.5, and 3.9 μm absorptions. Vertical lines are at 2.33 and 2.53 μm. Additional spectrum shown is from (c) clay- and carbonate-bearing materials exposed by $D \sim 19$ km central pit crater (7.8°S, 73.7°E). Red is D2300 parameter from CRISM FRT000064A8 on CTX P08_004207_1717 (no HiRISE imagery is available at this site).

4. Western Noachis Terra

Elsewhere on Mars (e.g., Figures 10 and 11), as described below, some spectra exhibit all the features described in section 3.1, except with a narrower 2.3 μm band centered at a shorter wavelength and deeper than the 2.5 μm band, the opposite proportions of those expected for carbonates (Figure 1, bottom spectrum). This suite of features is consistent with the secondary mineral component in the region being composed of carbonate (≤50%) mixed with Fe/Mg-smectite. As demonstrated by *Bishop et al*. [2013b], the ~2.3 μm band position is governed by the phyllosilicate to such an extent that even only 10% smectite (nontronite) intermixed with carbonate (magnesite) yields a nontronite-like band minimum at 2.28 μm. At smectite fractions above ~50%, the 2.3 μm absorption is ~2 times as deep as the 2.5 μm absorption, as observed here. The broad ~3 μm H_2O absorptions of phyllosilicates also reduce the spectral contrast of carbonates' ~3.4 μm features, but the latter nevertheless remains discernible when carbonate is equal or even a bit less abundant than smectite, as do the ~2.5 and ~3.9 μm absorptions [*Bishop et al*., 2013b]. Thus, we interpret spectra such as that shown in Figure 12a (same as Figure 1, bottom) as combinations of carbonates and

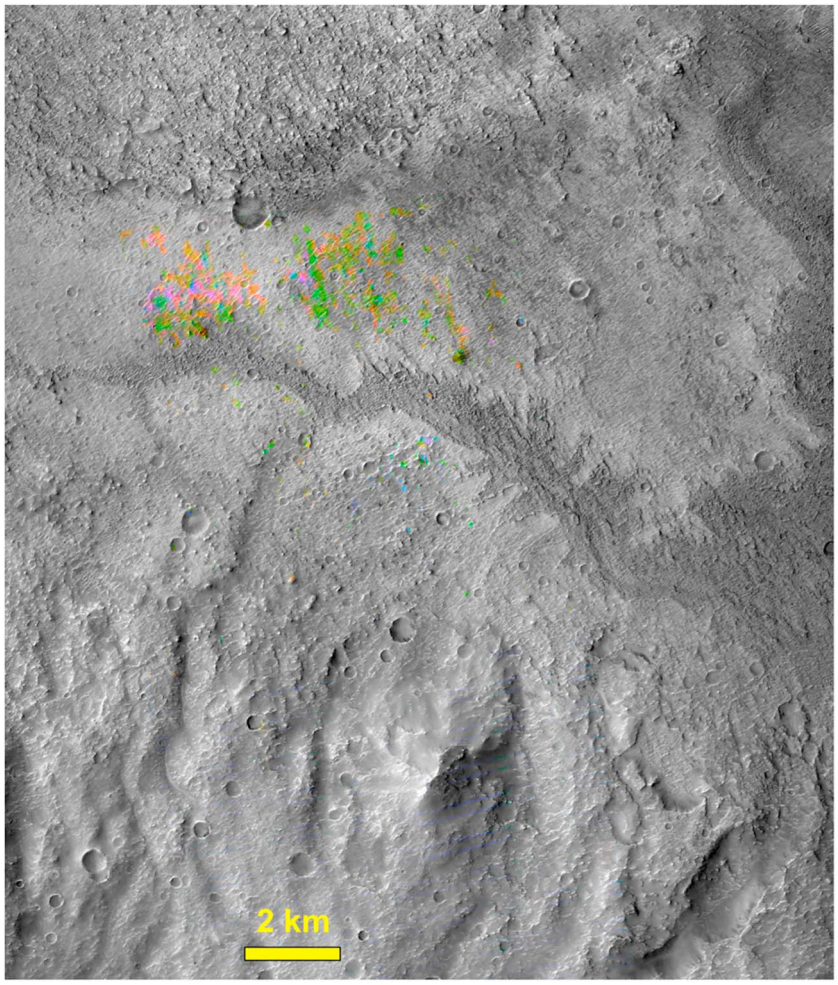

Figure 8. Clay + carbonate exposures surrounding digitate deposit on southern Huygens basin floor (southernmost arrow in Figure 2). CRISM HRL00024A8B overlain on CTX D15_033151_1625; R/G/B are the parameters OLINDEX/D2300/BDCARB from *Pelkey et al*. [2007]. The materials highlighted by the CRISM parameters have spectral absorptions at 1.92 μm (hydration), 2.30 and 2.52 μm, consistent with Fe/Mg-smectites mixed with carbonate of intermediate composition.

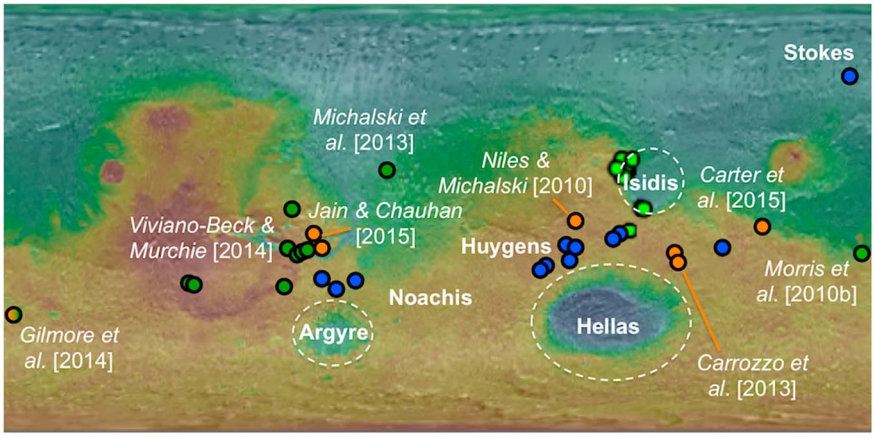

Figure 9. Carbonate-bearing rocks found on Mars to date, on MOLA topography (modified from *Ehlmann et al*. [2008]). Green points are Mg-carbonates (reported by *Ehlmann et al*. [2008], except where indicated), orange are Fe/Ca-carbonates reported by other authors, while dark blue points are newly reported here (consistent with Fe/Ca-carbonates, except for the Mg-carbonates inferred in Hesperia Planum and Stokes crater).

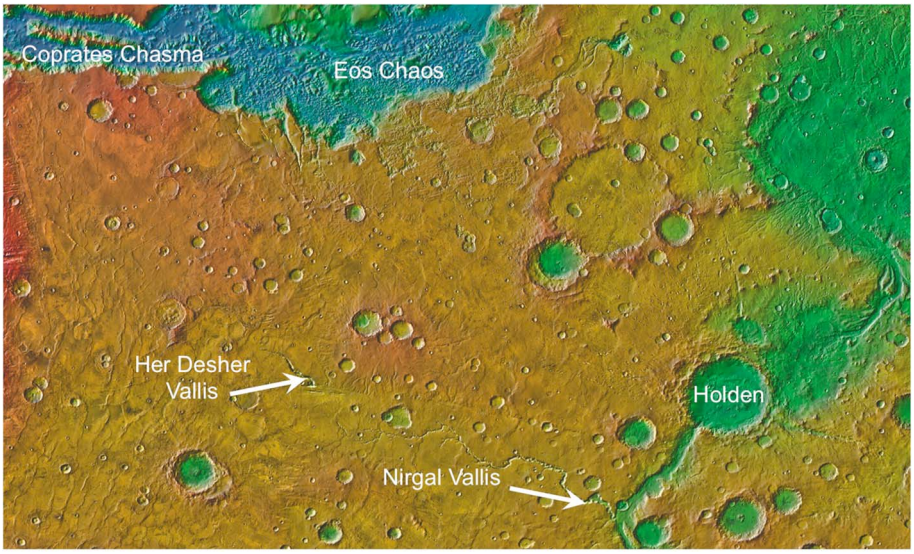

Figure 10. Plains and valleys west of Noachis Terra and the $D \sim 154$ km Holden crater. Arrows point to locations of clay + carbonate detection in Her Desher Vallis (CRISM HRL00009B61) and Nirgal Valllis (FRT0000C875). Background is MOLA topography colorizing THEMIS daytime IR mosaic.

clays, with Ca-carbonate best fitting the 2.54 and ~3.5 μm absorptions, while Fe/Mg-smectite, perhaps at equal or somewhat higher abundance, explains the narrower minimum at 2.30 μm, the weak absorption (as opposed to a carbonate-like peak) at ~2.4 μm, and the absorptions at 1.4, 1.9, and 3 μm.

The spectrum in Figure 12a and others like it are found in a region that we call "western Noachis Terra," constituting the plains west of Holden crater and the Uzboi-Ladon-Margaritifer Valles outflow system [*Grant and Parker*, 2002] and to the south of eastern Valles Marineris (Figure 10). This area hosts an extensive regional subsurface layer of Fe/Mg-phyllosilicates mapped by *Buczkowski et al*. [2010, 2013] and by *Le Deit et al*. [2012], dating to the Noachian period. This layer is tens of meters thick and is exposed continuously along impact crater rims, valley walls, and other locations throughout the region where erosion has revealed the subsurface stratigraphy [*Buczkowski et al*., 2010, 2013; *Le Deit et al*., 2012]. The spectrum in Figure 12a is from such an exposure along the walls of Her Desher Vallis (~26°S, 47°W). CRISM hyperspectral mapping shows that ~2.5 and ~3.9 μm absorptions consistent with carbonate span several kilometers of phyllosilicate-rich outcrop laterally at this location but are not ubiquitous within this layer (Figure 11). Indeed, although the extensive mapping completed by *Buczkowski et al*. [2010, 2013] and *Le Deit et al*. [2012] shows that the phyllosilicate layer may stretch hundreds or even >1000 km from Argyre basin to Valles Marineris, still at many locations its spectrum lacks a clear ~2.5 μm absorption. So carbonates may be present only locally, although we do identify them in at least one other outcrop of the phyllosilicate-bearing layer (~29°S, 38.5°W), ~500 km southeast of Her Desher along the walls of lower Nirgal Vallis (Figure 10).

Nirgal is a tributary of Uzboi Vallis, which flooded Holden crater during the Late Noachian or Early Hesperian epoch [*Grant et al*., 2008, 2010]. Clay-bearing, light-toned strata (Figure 13) interpreted as sublacustrine or distal alluvial deposits are found on Holden's floor [*Milliken and Bish*, 2010]. The strongest Fe/Mg-phyllosilicate signatures occur in strata that are inferred to predate Uzboi's breaching of the Holden crater rim [*Grant et al*., 2008], but the Uzboi flood deposits also show phyllosilicate signatures. Regardless, Holden itself may have excavated through the western Noachis Terra phyllosilicate layer and incorporated those materials into its early crater floor sediments. The lowermost sedimentary layer—labeled the lower unit, lower member in the stratigraphy of *Grant et al*. [2008]—has the strongest clay signatures [*Milliken and Bish*, 2010], consistent with ~25–45% phyllosilicates by volume [*Poulet et al*., 2014]. It is darker than the overlying strata and extensively jointed (Figure 14). In certain locations, it shows additional spectral features at the wavelengths at which carbonates absorb: a 2.5 μm absorption and a deeper, broader 2.3 μm band (Figure 14c). However, the 3–4 μm features are at the noise level (Figure 14d), and the shape and width of the 2.5 μm feature do not closely match the rounded, asymmetric 2.5 μm absorptions in our

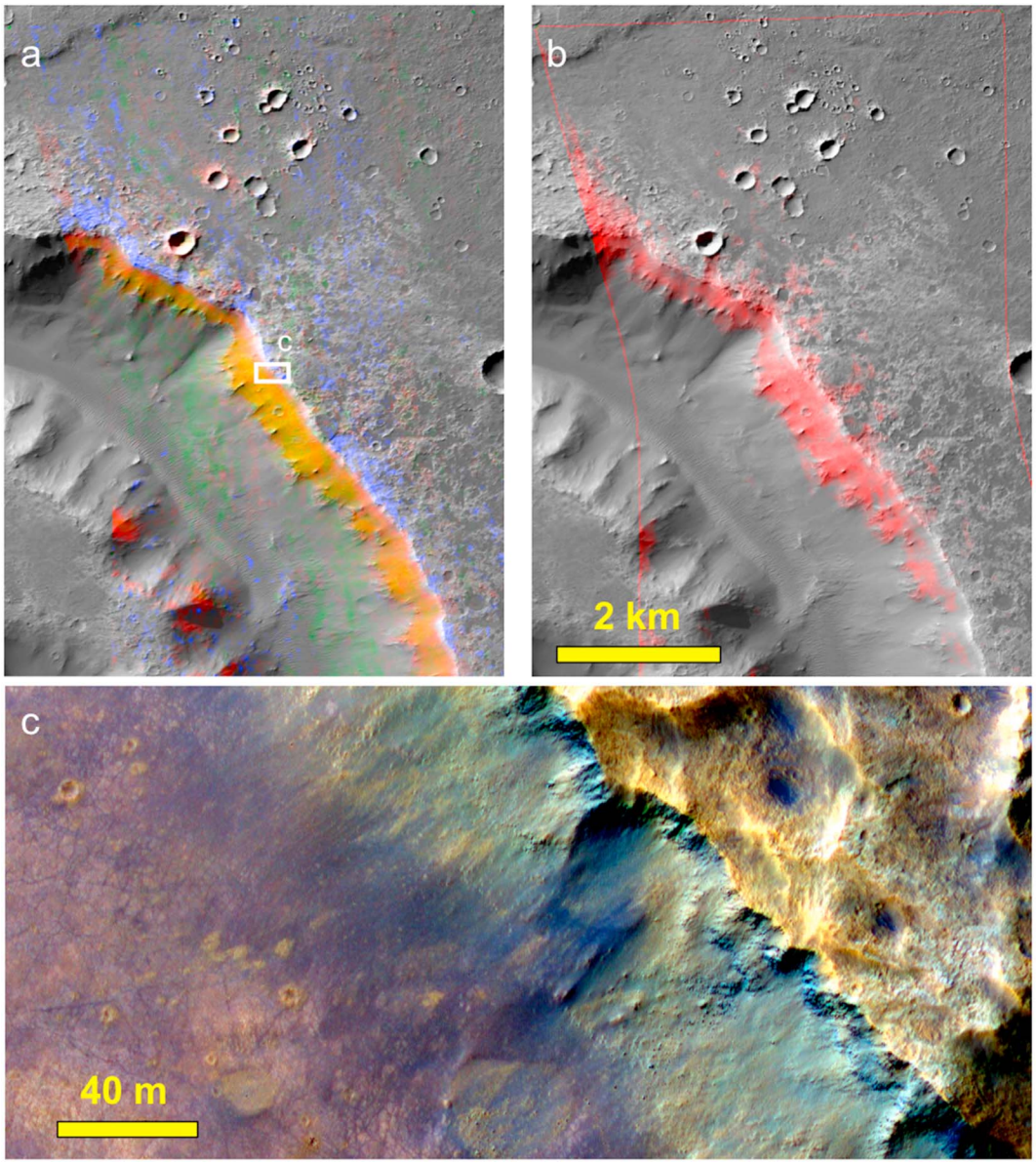

Figure 11. Aqueous minerals exposed in the upper wall of Her Desher Vallis. (a) A shallow subsurface layer mapped by *Buczkowski et al.* [2010, 2013] contains ubiquitous Fe/Mg-phyllosilicates (red), variably mixed with carbonate (yellow). This is overlain by a different hydrous mineral, possibly sulfate (blue). Red is D2300, green is BDCARB, blue is SINDEX [*Pelkey et al.*, 2007]; purely green (not yellow) areas are artifacts. CRISM HRL00009B61 overlain on CTX B20_017450_1542, as in (b) where carbonates are mapped independently using the CINDEX parameter [*Pelkey et al.*, 2007], tracking their 3.9 μm absorption (red). Note correspondence to all yellow areas in Figure 11a (i.e., spectra having both 2.3 and 2.5 μm absorptions), but not areas that are red in Figure 11a (i.e., having only a 2.3 μm band). (c) Enhanced color view [*Delamere et al.*, 2010] of the transition from hydrous (sulfate?) layer (bright blue to yellow hues) to underlying clay- and carbonate-bearing layers (darker maroon). Spectrum in Figure 12 was taken from left edge of this image and laterally equivalent materials spanning 308 CRISM pixels. The darker subunit at the top of the clay-bearing horizon extends for at least several kilometers and appears deficient in carbonate relative to the underlying, polygonally fractured outcrop. From HiRISE PSP_007086_1545_IRB.

laboratory carbonate spectra (Figure 1); these Martian spectra may be more consistent with an alteration assemblage dominated by smectite/chlorite mixed-layer clays [*Milliken et al.*, 2011]. Still, Holden was a sink for sediments that likely sampled the materials to its west that show stronger evidence for a carbonate component. The possibility of sampling carbonates adds to Holden's appeal as a candidate landing site for future Mars missions [*Golombek et al.*, 2012].

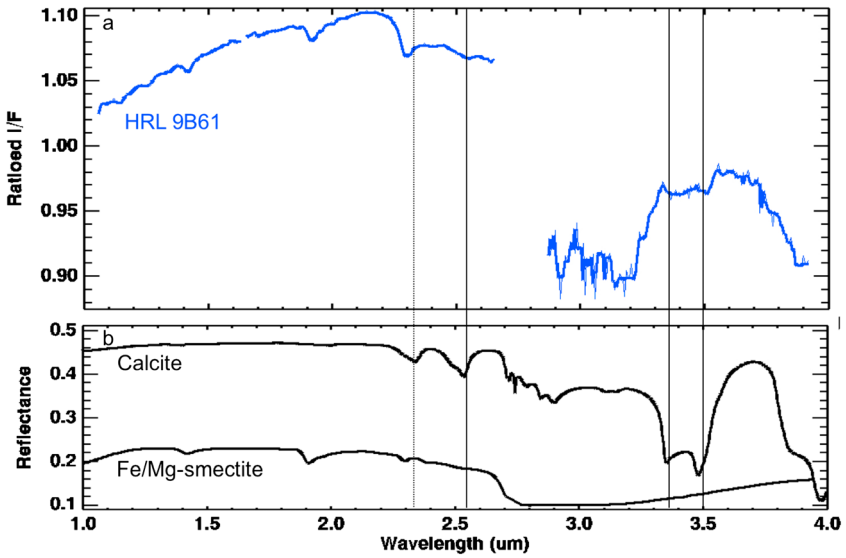

Figure 12. (a) Spectrum of shallow subsurface clays + carbonates; from CRISM HRL0009B61 covering a portion of Her Desher Vallis (see Figure 11 for location). (b) Laboratory calcite and smectite spectra for comparison; calcite is same as in Figure 1; smectite is sample GDS759A from Flagstaff Hill, CA (courtesy G. Swayze). Vertical lines are at 2.33, 2.54, 3.36, and 3.5 μm.

Beyond the northern edge of Figure 10, *Jain and Chauhan* [2015] explored CRISM observations in the Capri Chasma region and demonstrated evidence for Fe/Ca-carbonates. *Viviano-Beck and Murchie* [2014] have reported Mg-carbonates in Coprates Chasma and southward (west of Her Desher Vallis) in the Thaumasia highlands, while *Bultel et al.* [2015a] confirmed additional detections in Coprates Chasma. As with Huygens

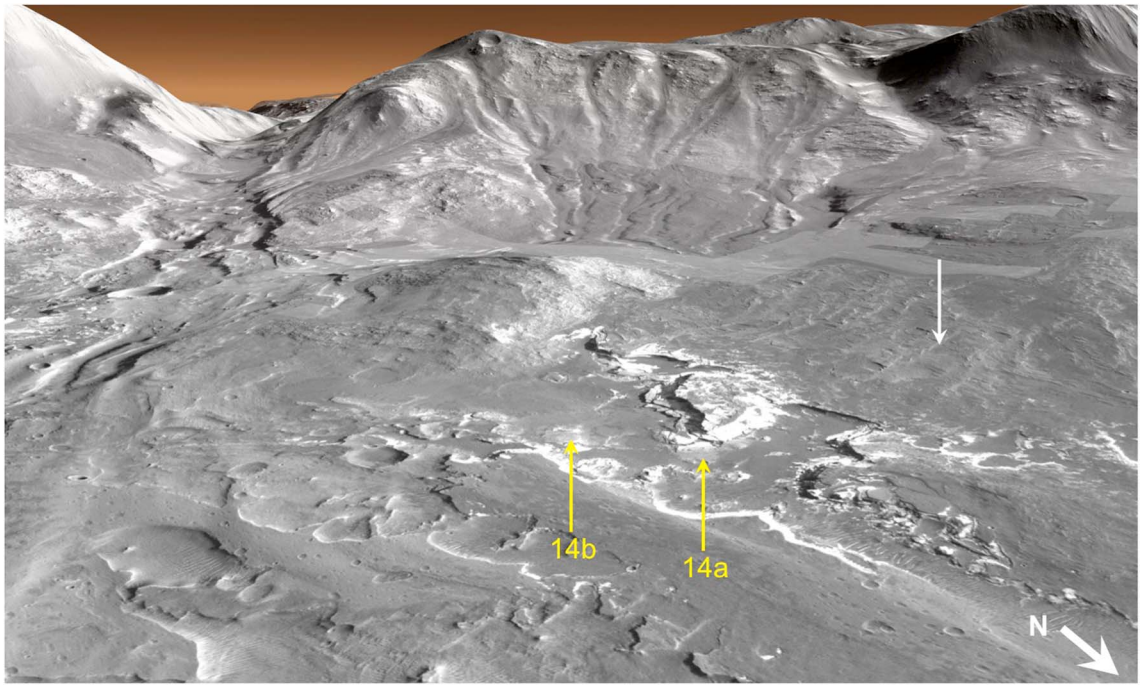

Figure 13. CTX image mosaic draped over MOLA topography (2 times exaggerated), looking southwest from within Holden crater (26°S, 326°E; D~154 km) toward where Uzboi Vallis breaches its rim (upper left). Light-toned layered deposits on the crater floor contain clay minerals (yellow arrows), with an additional component that varies spatially and may be carbonate. At middle right, the darker, smoothly sloping surface with inverted distributary channels (white arrow) is the alluvial bajada proposed as a landing site for Mars Science Laboratory's Curiosity rover [*Grant et al.*, 2011]. Screenshot taken from Google Mars.

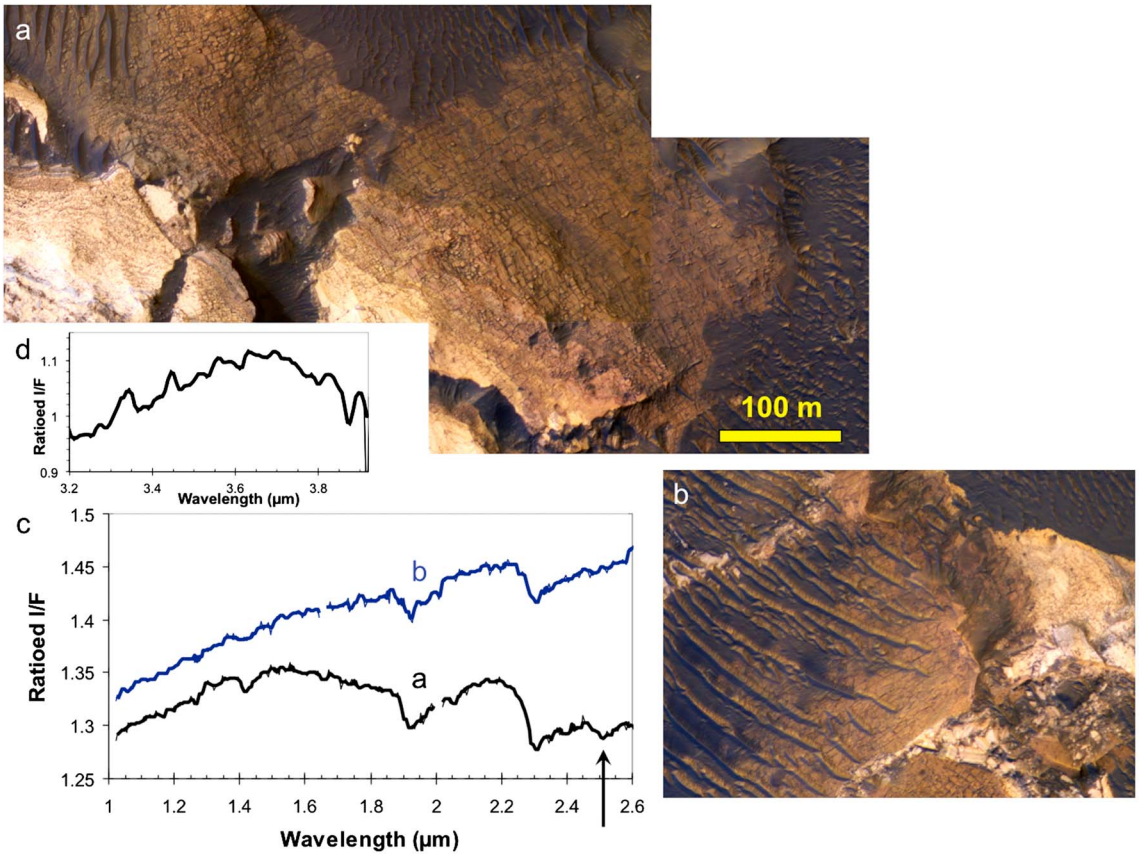

Figure 14. Lower member of the lower unit in Holden crater floor stratigraphy. (a) Outcrop possibly containing carbonate; mosaic of HiRISE PSP_002088_1530_IRB (upper left) and ESP_019256_2030_IRB data. (b) Clay-bearing outcrop with no clear evidence for carbonate; from ESP_019256_2030_IRB, with scale same as in Figure 14a. (c) Spectra of outcrops Figures 14a and 14b from CRISM FRT0000C1D1 (averages of 418 and 268 pixels, respectively). Arrow indicates a 2.5 μm absorption found only in Figure 14a, which also has a stronger 3.9 μm band and a (d) ~3.5 μm region more consistent with carbonate than in Figure 14b.

basin and its surroundings, this is a visually striking cluster of spectrally similar materials (Figure 9), but whether all are genetically related is unknown.

5. Other Locations

We describe here a few additional carbonate or possible carbonate detections scattered across Mars, in the interest of constraining their global distribution to the extent currently possible (Figure 9). Our ability to do so is limited by the spatial coverage of existing targeted observations and the incompleteness of our survey of them.

In eastern Hesperia Planum, a $D \sim 42$ km crater at 119.6°E, 13.6°S exposes material consistent with Mg-carbonate plus Fe/Mg-phyllosilicates on its pitted central peak (Figure 15). This central uplift exhibits considerable diversity in visible-wavelength color (Figure 15b) and includes exposures of chlorite, Al-phyllosilicates, and other hydrated minerals. In some uplifted blocks that are themselves layered, all four spectral features of carbonates are identified (and spatially correlated), although superposed on a strong overall "blue" slope (i.e., lower reflectivity at longer wavelengths); Figure 15d plots spectral ratios, but we have confirmed that this blue slope is intrinsic to the numerator pixels. Such blue slopes, accompanied by broad absorptions centered at ~1.2 μm (which we also observe), have elsewhere on Mars been attributed to weathering or silica-rich rinds developed on basaltic glass [*Mustard et al.*, 2005; *Horgan and Bell*, 2012]. In the Hesperia crater context, they might represent a weathered version of the impact glasses recently reported by *Cannon and Mustard* [2015]. In any case, continuum-removed spectra clearly show rounded 2.30 and 2.50 μm absorptions that are of comparable strength in some outcrops, consistent with Mg-carbonate, while in other locations the 2.3 μm band is stronger and other features (e.g., a 1.4 μm absorption) indicate mixture with Fe/Mg-phyllosilicates

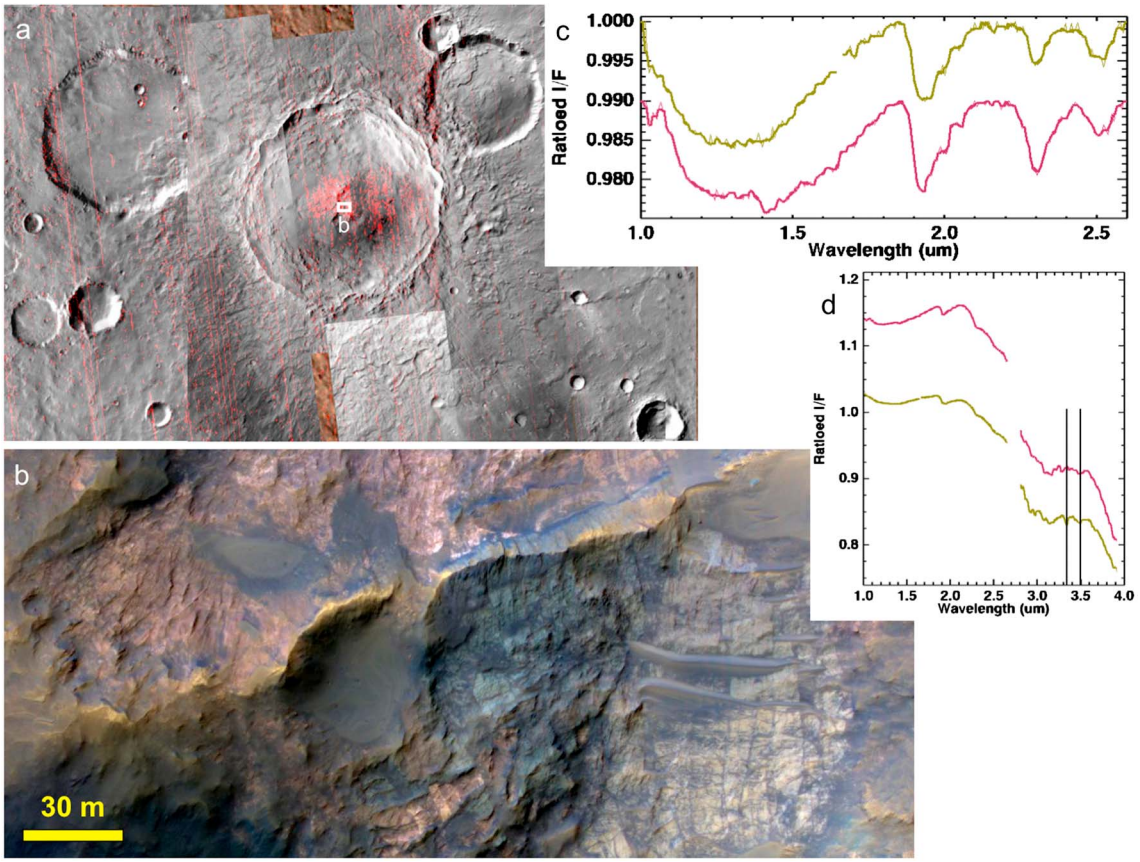

Figure 15. Unnamed $D \sim 42$ km crater in eastern Hesperia Planum with clay + carbonate exposed on its central peak (corresponds to unlabeled point northeast of Hellas in Figure 9). (a) CRISM multispectral data (D2300 parameter in red) superposed on mosaic of CTX, THEMIS daytime IR, and Viking image data. Red stripes aligned with the MRO ground track are systematic artifacts, but other red areas contain carbonates and/or Fe/Mg-phyllosilicates. (b) Layered or foliated rocks of mixed composition including Mg-carbonate (concentrated in the lighter-toned rocks at right), Fe/Mg-clay (concentrated in redder materials to the left), and possibly weathered glass; from HiRISE ESP_025105_1665_IRB. (c) Continuum-removed spectral averages of 724 pixels centered on the material in Figure 15b (maroon, vertically offset) and 228 pixels from a more carbonate-dominated mound ~1.5 km away (gold—note weaker 2.3 μm band and absence of 1.4 μm band). From CRISM FRT00007DF8. (d) The same two spectral averages prior to continuum removal, showing broad blue slopes that extend to the longest wavelengths measured by CRISM.

(Figure 15c). Additional CRISM imaging in and around this crater shows that these signatures are localized to the central uplift and the adjacent crater floor and not found in the crater's reasonably well-preserved ejecta (Figure 15a). Secondary minerals having this spatial distribution could be consistent with being the deepest preexisting material excavated here, reaching the surface only in the structurally uplifted central peak (~4.5 km estimated preimpact burial depth), but alternatively could have resulted from impact-induced hydrothermal alteration.

Another carbonate detection, albeit slightly less definitive, occurs in Stokes crater on the northern plains of Mars (55.6°N, 171°E). The mineralogy of this $D \sim 63$ km crater's central uplift, which also exposes primary mafic silicates and several different types of phyllosilicates, was described in detail by *Carter et al*. [2010]. Here we note the additional observation of some outcrops (~7 km estimated preimpact burial depth) on which the 1.9 and 2.3 μm phyllosilicate absorptions are accompanied by a rounded absorption at ~2.51 μm and a dropoff toward 3.9 μm (Figure 16), consistent with Mg-carbonate. In this case, no features at ~3.4–3.5 μm are clearly visible above the noise in the data. However, detecting those features in association with strongly hydrated phases (which have major 3 μm H_2O bands) is inherently difficult [e.g., *Harner and Gilmore*, 2015]. Stokes crater therefore illustrates how requiring all four carbonate spectral features as criteria for detection, while minimizing false positives could in principle lead to underestimation of how widespread carbonates actually are in altered Noachian crustal materials. We have made similar possible detections in the Eridania basin

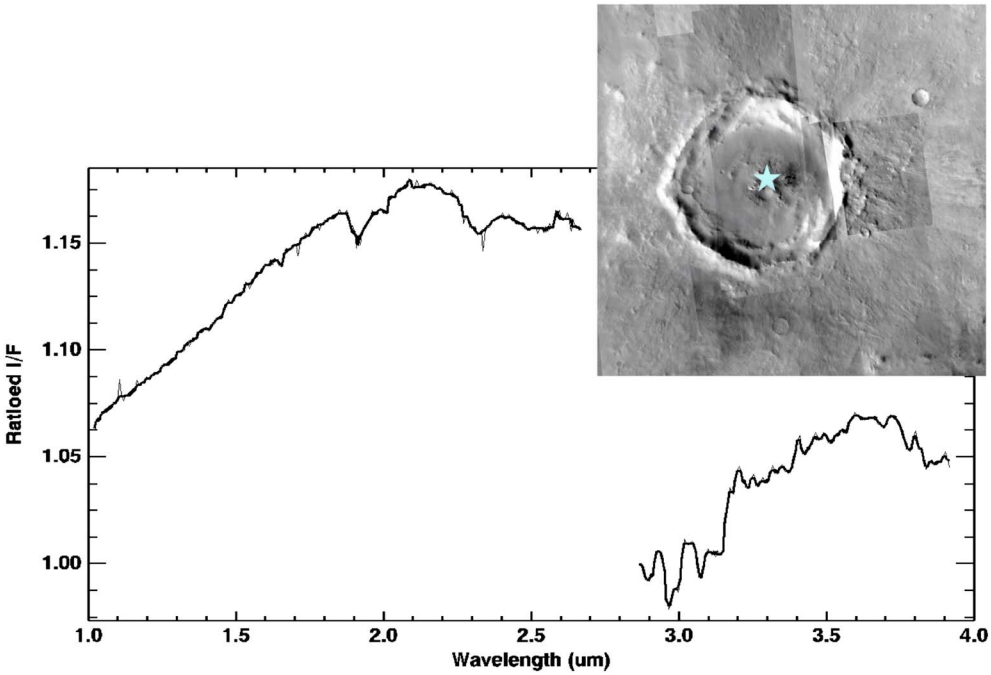

Figure 16. Stokes crater (56°N), which is 63 km in diameter. Inset is a CTX image mosaic, with star marking the source location for the spectrum (a 138 pixel average from CRISM FRT0000ADA4).

(CRISM FRT0000989C) and cooccurring with Fe/Mg-smectite clays cropping out on knobs in the Icaria Fossae region southwest of Tharsis [e.g., *Wray et al*., 2009, Figure 3c]. The Stokes crater outcrop is especially interesting given its distance from other carbonate-bearing rocks reported to date (Figure 9) and its implication that carbonate bedrock formed in both Martian hemispheres prior to the emplacement of the northern plains, similar to clay formation [*Carter et al*., 2010].

6. Discussion

The detections described in this paper expand the geographic distribution of known carbonate-bearing rocks on Mars and suggest that conditions suitable for Fe/Ca-carbonate formation were widespread at least regionally. It remains unclear whether such conditions were truly global. A recent review concluded that local hydrothermal environments would have been sufficient to produce most of the carbonates found to date [*Niles et al*., 2013]; evidence from both meteorites [e.g., *Halevy et al*., 2011] and geochemical modeling of the remotely sensed assemblages [*Van Berk and Fu*, 2011] suggests moderate temperatures (tens of °C) for such systems. *Romanek et al*. [2009] showed that Mg incorporation into mixed-cation carbonates is much less effective at 25°C than at 70°C, which would be consistent with the Mg-rich carbonates on Mars having a higher-temperature origin than those appearing Fe/Ca-rich. Alternatively, the Fe/Ca-carbonates could have formed from more dilute waters, whereas the more soluble Mg-carbonates could record locations of later brines more concentrated by evaporative or cryogenic processes [*Hardie and Eugster*, 1970; *Tosca and McLennan*, 2006]. In either case, siderite in particular implies formation from surface or subsurface fluids with higher [Fe^{2+}]—and therefore a less oxidizing environment—than the surfaces of modern Earth or Mars [e.g., *Catling*, 1999; *Niles et al*., 2013].

Unlike other proposed solid sinks for Martian carbon such as oxalates (Figure 17), at low spectral resolution carbonates can be difficult to distinguish from Fe/Mg-phyllosilicates in the near-IR, especially when the two occur in mixtures [e.g., *Bishop et al*., 2013b]. Indeed, the Lucaya crater carbonate outcrop was initially identified as a "phyllosilicate exposure" based on CRISM multispectral data. (The original multispectral set of wavelengths does not sample the ~2.5 μm region adequately to separate carbonate from Fe/Mg-phyllosilicates definitively.) *Wray et al*. [2009] reported ~10^2 new exposures of Fe/Mg-phyllosilicate in the southern highlands, and thousands of such exposures were reported in the highlands by *Mustard et al*.

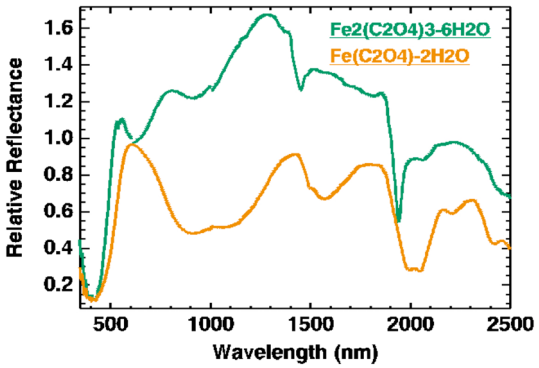

Figure 17. Spectra of two Fe-oxalate minerals proposed by *Eigenbrode et al.* [2014] and *Niles et al.* [2015] as possible alternative carbon sinks in Martian soil. Their IR spectral features are notably distinct from those of carbonates or Fe/Mg-phyllosilicates, lacking ~2.3 μm features but with distinctive absorptions at ~1.6 and 2 μm (ferrous) or ~0.6 μm (ferric). Oxalate powders from Sigma-Aldrich were measured with a Spectral Evolution PSR-3500 spectrometer at the Georgia Institute of Technology.

[2008], *Murchie et al.* [2009a], *Ehlmann et al.* [2011], and *Carter et al.* [2013]. Some of these may, in fact, be mixtures of carbonate + phyllosilicate; where possible, detailed analysis of follow-up hyperspectral observations to distinguish carbonate from phyllosilicate at these locations would be illuminating. By analogy to many of the exposures reported herein, the central uplifts and walls of midsized to large craters should be prime targets in the search for additional Fe/Ca-carbonates.

The association of Fe/Ca-carbonates with complex craters—including Leighton [*Michalski and Niles*, 2010] and those around the Huygens basin—suggests impact-related formation and/or exposure of previously buried carbonate. If carbonates formed in the subsurface after their host rocks were buried, then this would have required CO_2-rich fluids to be present at ~5 km depth and to precipitate carbonate without the facilitative effect of depressurization-induced supersaturation that occurs if such fluids reach the surface through groundwater upwelling [e.g., *Pentecost*, 1995; *Michalski et al.*, 2013]. *Michalski and Niles* [2010] considered this subsurface carbonation scenario less likely because it is unclear if sufficient CO_2 could be transported to ~6 km depth via fluids descending from the surface. Carbonates occur in impact hydrothermal assemblages on Earth, but unless the target rocks contained abundant carbonates as in the Haughton and Ries impacts [e.g., *Osinski*, 2003; *Osinski et al.*, 2001, 2004, 2005], they are typically a relatively minor component (~1–2% or less) of the impactites (e.g., Lonar crater) [*Hagerty and Newsom*, 2003]. Carbonates predating an impact, if not lost via devolatilization [*Hörz et al.*, 2015], generally remain spectrally detectable as such following the impact [*Cloutis et al.*, 2010]. We therefore infer that carbonates likely existed in the subsurface around Huygens prior to the impacts that exposed (and possibly modified) them. Indeed, the presence of these carbonates in Huygens rim rocks suggests that they predate Huygens itself, an Early Noachian basin dated to ~3.98 Ga [*Werner*, 2008], in which case they would also predate the Late Noachian Mg-carbonates near Isidis [*Ehlmann et al.*, 2008, 2009; *Bishop et al.*, 2013a] and layered phyllosilicates across Mars [e.g., *Murchie et al.*, 2009a; *Ehlmann et al.*, 2011]. In fact, Huygens likely impacted the slightly older ejecta of nearby Hellas basin, defined as the base of the Noachian [*Carr and Head*, 2010], so materials buried ~5 km at this location may well be pre-Noachian. This age relation would be consistent with evidence presented by *Glotch and Rogers* [2013] for decomposition products of Ca-carbonates spread across the Syrtis region, which they interpreted as evidence for a vast regional, deep Early- to Mid-Noachian carbonate unit there. Early burial could have protected these carbonates from later decomposition due to surface acidity [*Bibring et al.*, 2006], helping to explain why few large exposures of carbonate-rich rocks have been identified. Unlike Earth, Mars has no plate tectonic system to raise deeply buried materials to the surface; only rare large impacts or faulting do so. We continue to search for additional exposures, although the oldest Martian rocks are often highly brecciated [*McEwen et al.*, 2008] at scales that challenge the spatial resolution of CRISM.

Carbonates in Noachis Terra cooccur with layered phyllosilicates in the shallow subsurface and could be younger. In fact, this horizon appears above and may postdate [*Buczkowski et al.*, 2013] a regional sequence of Al-phyllosilicates overlying Fe/Mg-phyllosilicates dated near the Late Noachian/Early Hesperian boundary [*Murchie et al.*, 2009a; *Le Deit et al.*, 2012]. This relatively late age is consistent with the stratigraphic placement of other clays in this region (Uzboi-Ladon-Morava basin system) according to *Grotzinger and Milliken* [2012], who noted that other parts of the planet were forming sulfates under possibly more acidic conditions by that time. Fluids across this region may have remained nonacidic longer than elsewhere on Mars, allowing both the carbonates and clays to persist and be fluvially transported to regional basins. Ritchey crater formed within this region and provides further evidence for post-Noachian conditions conducive to clay formation here [*Sun and Milliken*, 2014]. However, polyhydrated sulfates have recently been found associated with the Noachis phyllosilicate horizon; their distribution is heterogeneous, and they appear more common closer

to the Tharsis volcanoes, which could have been a sulfur source (D. L. Buczkowski et al., manuscript in preparation, 2015). No outcrops hosting both carbonate and sulfate have yet been found, consistent with the hypothesis that sulfates trace locations where acidic fluids could have destroyed preexisting carbonates.

Is the global distribution of carbonate-bearing rock detections (Figure 9) a product of any process(es) less stochastic than impact (or tectonic) exposures of subsurface carbonates? It may be significant that most of our new carbonate detections occur near the three largest well-preserved impact basins on Mars (within one basin radius of Argyre, Hellas, and/or Isidis; Figure 9). At Isidis, in particular, the largest exposures of olivine-rich outcrop on Mars were interpreted by *Mustard et al*. [2007] as melt from the basin-forming impact, which would have excavated lower crustal and possibly upper mantle materials. Olivine may be an important precursor for Mg-carbonates [e.g., *Ehlmann et al*., 2008; *Brown et al*., 2010], and as discussed by *Niles and Michalski* [2009], it is also true more generally that interaction with mafic/ultramafic crust should neutralize aqueous fluids and prevent acidic weathering/inhibition of carbonates; such neutralization may have been most effective in olivine-rich regions. Indeed, our areas of spatially clustered carbonates in western Noachis Terra and the circum-Isidis/Terra Tyrrhena region loosely correlate with clusters of olivine exposures [e.g., *Ehlmann and Edwards*, 2014, Figure 2a], although a concentration specifically surrounding Huygens basin northwest of Hellas is not observed.

One striking attribute of the region northwest of Hellas is its major element chemistry inferred from gamma ray spectra. *Karunatillake et al*. [2009] referred to this area as "chemically striking region" #5, characterized by broad-scale depletion in Fe and enrichment in Al by at least one standard deviation relative to their global average values; the Al enrichment extends farther northward to the west of Syrtis Major. Si is also enriched in this region, with all of these chemical trends being consistent with the recent inference of widespread felsic (mafic-poor, feldspar-rich) materials in this region [*Wray et al*., 2013]. These attributes might appear irrelevant if they were not also shared by western Noachis Terra; it is a chemically striking region (#70 of *Karunatillake et al*. [2009]) again characterized by Si enrichment—with its northerly half also enriched in Al—and it is the other area on Mars where felsic materials have been detected [*Carter and Poulet*, 2013, Figure 1b]. In fact, these are the only two major Si-enriched areas of the Martian highlands [*Karunatillake et al*., 2009]; the only other broad Si enrichments are found in the northern lowland terrains spectrally dominated by "TES surface type 2" (see *Karunatillake et al*. [2006] for further discussion). These two highland regions also have lower remotely sensed sulfur abundances than the recent rover landing sites in Meridiani Planum or Gale and Gusev craters [*Karunatillake et al*., 2014]. In light of models for generating surface acidity that involve oxidation of iron and/or sulfur [e.g., *Burns*, 1993; *Zolotov and Shock*, 2005; *Baldridge et al*., 2009; *Hurowitz et al*., 2010], we speculate that lesser availability of sulfur and/or divalent cations in these regions—whether because of different crustal primary compositions or greater extent of prior weathering—reduced the acidity of the Late Noachian to Early Hesperian ground and surface waters regionally and thus allowed greater preservation of carbonates. The Si and Al enrichments could alternatively reflect regional phyllosilicate deposition, which would also be consistent with a neutral-to-alkaline environment that could additionally host carbonates.

Martian carbonates may provide a valuable standard for interpreting any organics found on Mars [e.g., *Freissinet et al*., 2015], because while it is likely that biological processes would fractionate carbon isotopes differently from abiotic processes [*Webster and Mahaffy*, 2011], such fractionation can only be meaningfully quantified and interpreted through comparison to a coeval Martian inorganic "standard" [*Summons et al*., 2011]. Therefore, in order to seek on Mars the isotopic biosignatures that provide our most ancient evidence for life on Earth [*Rosing*, 1999], it may be critical to examine ancient carbonates. Even if habitable environments were largely restricted to the Martian subsurface [e.g., *Ehlmann et al*., 2011], buried carbonates could have provided a source of carbon for metabolism in the deep crust isolated from atmospheric CO_2 [*Kral et al*., 2014]. For all of the above reasons, understanding carbonates is a key part of understanding the Martian carbon cycle [*Grady and Wright*, 2006].

Grotzinger et al. [2015] interpreted Curiosity's observations in Gale crater to indicate an early Martian climate that allowed stable water lakes at the Martian surface for thousands to millions of years at a time. While debate continues regarding the climatic implications of >1 bar CO_2 in the Martian paleoatmosphere [e.g., *Kasting*, 1991; *Forget and Pierrehumbert*, 1997; *Forget et al*., 2012; *Urata and Toon*, 2013; *Ramirez et al*., 2014], it is nevertheless of interest to determine whether the observed carbonates are consistent with a reservoir sizable enough to hold a large fraction of such an atmosphere. There is no other obvious sink for such a

reservoir; *Zent and Quinn* [1995] concluded that only up to ~30–40 mbar CO_2 could be adsorbed in the regolith, and the recently discovered CO_2 buried in the South Polar Layered Deposits adds only ~5 mbar more [*Phillips et al*., 2011]. Considering the various mechanisms for atmospheric loss to—or gain from—space, *Lammer et al*. [2013] concluded that only ~100 mbar could have been lost over the past ~4 Gyr. Furthermore, *Goldspiel and Squyres* [1991] noted that the visible paleolake basin deposits could store only a few millibars of carbonates, and *Goudge et al*. [2012, 2015] have since shown that most of these do not contain any detectable carbonates. Therefore, buried ancient basins appear the only remaining option, but how widespread carbonates are in the subsurface remains a critical unknown. For example, *Warren* [1987] noted that a carbonate global equivalent layer of ~20 m thickness could store ~1 bar of CO_2. The Huygens carbonate-bearing deposits exposed in Lucaya crater have a ~50 m thickness, so if this layer extended globally, it could store ~1 bar of CO_2 with only a ~40% carbonate abundance by volume. Given the presence of cooccurring phyllosilicates while carbonate nonetheless dominates the ~2.3 μm region, 40% carbonate is a reasonable estimate [*Bishop et al*., 2013b]. At the other extreme, if Lucaya's carbonate layer spans only the entire area of Huygens crater (but is only exposed at the locations observed), then it would represent a reservoir more comparable to that estimated for Nili Fossae by *Edwards and Ehlmann* [2015]; most likely a few millibars, or potentially up to double this amount if additional outcrops surrounding the Isidis basin are also included [*Viviano-Beck*, 2015]. The true Martian carbonate reservoir may be somewhere in between these two end-members; e.g., *Hu et al*. [2015] model a few hundreds of millibars of Late Noachian/Hesperian carbonates in order to explain the observed atmospheric C isotope ratios. On the other hand, Huygens and its associated carbonates are older than the period modeled by *Hu et al*. [2015], and could therefore represent a reservoir for Mars' earliest atmosphere [*Jakosky and Jones*, 1997].

In summary, estimates of Mars' buried carbon reservoir must for now rely upon tenuous assumptions about the global versus regional nature of deep carbonates. A systematic global search for carbonates using their 2.5 μm absorption and the oft-neglected 3–4 μm range would better constrain their distribution. In fact, a systematic survey of carbonates in highland crater walls and central peaks is one objective of MRO's third extended mission, currently ongoing. In addition, advances in CRISM data processing make detection of carbonates easier, particularly the new Map-projected Targeted Reduced Data Records (MTRDRs). As described by *Seelos et al*. [2011, 2012], MTRDRs include corrections for several systematic issues such as spectral smile (the cross-track shift in wavelength calibration across a scene) and artifacts related to the variable atmospheric path length within an observation. In addition, recently improved spectral summary parameters (e.g., CINDEX2) will allow better automated discrimination of carbonates from other alteration phases [*Viviano-Beck et al*., 2014].

7. Conclusions

The surface of Mars hosts a greater number and diversity of carbonate-bearing outcrops than was recognized prior to the high spatial resolution of observations made possible by CRISM. Some ~2000 km south of where the first, Mg-rich carbonate-bearing rocks were identified in Nili Fossae, the Noachian Huygens basin exposes Fe- and/or Ca-rich carbonates that cooccur with phyllosilicates in materials exposed by impact or transported down onto the basin floor. These carbonate-bearing rocks appear layered, and at least some were likely once buried several kilometers or more beneath the surface. Their occurrence across a region >2000 km wide implies that the layered Fe/Ca-carbonate found in Leighton crater's central uplift by *Michalski and Niles* [2010] is but one of many windows into a record of possibly widespread, neutral-to-alkaline aqueous conditions during the pre-Noachian period, preserved mostly in the subsurface.

On the other side of Mars, another regional set of Fe/Ca-carbonate exposures is found in western Noachis Terra. These carbonates also cooccur with phyllosilicates, apparently in heterogeneous proportions, in a layer tens of meters thick that may have provided sediments to the Holden crater paleolake. These and other examples of cooccurring clays and carbonates prompt questions about the degree to which the ubiquity of phyllosilicates in altered Noachian materials—and/or subsequent acidic weathering—may have spectrally obscured evidence of carbonates in all but the most carbonate-rich locations. In any case, these Fe/Ca-carbonates—especially the Early Noachian outcrops surrounding Huygens basin—may have formed in different geochemical environments from the Late Noachian Mg-carbonate-bearing rocks that have been more thoroughly studied to date. Their potential significance for tracing the history of Martian environments and gaining new astrobiological insights motivates further attention with upcoming orbital and landed missions to Mars, perhaps including eventual exploration by humans [*Ackiss et al*., 2015].

Acknowledgments
We thank the Mars Reconnaissance Orbiter HiRISE and CRISM instrument teams for acquiring critical data and for their financial, scientific, and collegial support. All HiRISE images used herein are publicly available at http://uahirise.org and all CRISM images at http://crism-map.jhuapl.edu. All other Mars data sets are accessible via the Google Mars interface. Fe-oxalate mineral spectra and CRISM regions of interest are available from the corresponding author upon request. J.J.W.'s work on this project was supported in part by the NASA Astrobiology Institute's SETI Institute node (grant 15BB01). Scientific discussions with Sheridan Ackiss, Veronica Bray, Debra Buczkowski, Roger Clark, Dick Morris, Eldar Noe Dobrea, Gregg Swayze, and Christina Viviano-Beck improved the paper. We thank Paul Niles and an anonymous reviewer for their detailed technical feedback, which strengthened the paper.

References

Ackiss, S. E., K. D. Seelos, and D. L. Buczkowski (2013), Mineralogic mapping of Huygens crater, Mars: A transect of the highlands crust and Hellas basin rim, Lunar Planet. Inst. Contrib., 1737, Abstract 3095.

Ackiss, S. E., J. J. Wray, K. D. Seelos, and P. B. Niles (2015), Huygens crater: Insights into Noachian volcanism, stratigraphy, and aqueous processes, Lunar Planet. Inst. Contrib., 1879, Abstract 1032.

Adler, H. H., and P. F. Kerr (1962), Infrared study of aragonite and calcite, *Am. Mineral.*, *47*, 700–717.

Adler, H. H., and P. F. Kerr (1963), Infrared absorption frequency trends for anhydrous normal carbonates, *Am. Mineral.*, *48*, 124–137.

Alzate, N., and N. G. Barlow (2011), Central pit craters on Ganymede, *Icarus*, *211*, 1274–1283, doi:10.1016/j.icarus.2010.10.015.

Applin, D. M., E. A. Cloutis, and M. R. M. Izawa (2014), Reflectance spectroscopy of hydrated carbonate minerals, Lunar Planet. Sci., XLV, Abstract 1881.

Applin, D. M., M. R. M. Izawa, E. A. Cloutis, D. Goltz, and J. R. Johnson (2015), Oxalate minerals on Mars?, *Earth Planet. Sci. Lett.*, *420*, 127–139, doi:10.1016/j.epsl.2015.03.034.

Archer, P. D., Jr., et al. (2014), Abundances and implications of volatile-bearing species from evolved gas analysis of the Rocknest aeolian deposit, Gale Crater, Mars, *J. Geophys. Res. Planets*, *119*, 237–254, doi:10.1002/2013JE004493.

Baldridge, A. M., S. J. Hook, J. K. Crowley, G. M. Marion, J. S. Kargel, J. L. Michalski, B. J. Thomson, C. R. de Souza Filho, N. T. Bridges, and A. J. Brown (2009), Contemporaneous deposition of phyllosilicates and sulfates: Using Australian acidic saline lake deposits to describe geochemical variability on Mars, *Geophys. Res. Lett.*, *36*, L19201, doi:10.1029/2009GL040069.

Bandfield, J. L., T. D. Glotch, and P. R. Christensen (2003), Spectroscopic identification of carbonate minerals in the Martian dust, *Science*, *301*, 1084–1087.

Beck, P., J. A. Barrat, P. Gillet, M. Wadhwa, I. A. Franchi, R. C. Greenwood, M. Bohn, J. Cotten, B. van de Moortèle, and B. Reynard (2006), Petrography and geochemistry of the chassignite Northwest Africa 2737 (NWA 2737), *Geochim. Cosmochim. Acta*, *70*, 2127–2139, doi:10.1016/j.gca.2006.01.016.

Benner, S. A., K. G. Devine, L. N. Matveeva, and D. H. Powell (2000), The missing organic molecules on Mars, *Proc. Natl. Acad. Sci. U.S.A.*, *97*(6), 2425–2430, doi:10.1073/pnas.040539497.

Bibring, J.-P., et al. (2006), Global mineralogical and aqueous Mars history derived from OMEGA/Mars Express data, *Science*, *312*, 400–404, doi:10.1126/science.1122659.

Bishop, J. L., J. F. Mustard, C. M. Pieters, and T. Hiroi (1998a), Recognition of minor constituents in reflectance spectra of Allan Hills 84001 chips and the importance for remote sensing of Mars, *Meteorit. Planet. Sci.*, *33*, 693–698.

Bishop, J. L., C. M. Pieters, T. Hiroi, and J. F. Mustard (1998b), Spectroscopic analysis of Martian meteorite Allan Hills 84001 powder and applications for spectral identification of minerals and other soil components on Mars, *Meteorit. Planet. Sci.*, *33*, 699–707.

Bishop, J. L., et al. (2013a), Mineralogy and morphology of geologic units at Libya Montes, Mars: Ancient aqueously derived outcrops, mafic flows, fluvial features, and impacts, *J. Geophys. Res. Planets*, *118*, 487–513, doi:10.1029/2012JE004151.

Bishop, J. L., K. A. Perry, M. D. Dyar, T. F. Bristow, D. F. Blake, A. J. Brown, and S. E. Peel (2013b), Coordinated spectral and XRD analyses of magnesite-nontronite-forsterite mixtures and implications for carbonates on Mars, *J. Geophys. Res. Planets*, *118*, 635–650, doi:10.1002/jgre.20066.

Bishop, J. L., D. Loizeau, N. K. McKeown, L. Saper, M. D. Dyar, D. J. Des Marais, M. Parente, and S. L. Murchie (2013c), What the ancient phyllosilicates at Mawrth Vallis can tell us about possible habitability on early Mars, *Planet. Space Sci.*, *86*, 130–149, doi:10.1016/j.pss.2013.05.006.

Bishop, J. L., S. J. King, A. J. Brown, and J. J. Wray (2015), Investigating the chemistry of Martian carbonates using CRISM data, Astrobiol. Sci. Conf., Abstract 7285.

Blaney, D. L., and T. B. McCord (1989), An observational search for carbonates on Mars, *J. Geophys. Res.*, *94*(B8), 10,159–10,166, doi:10.1029/JB094iB08p10159.

Booth, M. C., and H. H. Kieffer (1978), Carbonate formation in Marslike environments, *J. Geophys. Res.*, *83*(B4), 1809–1815, doi:10.1029/JB083iB04p01809.

Borg, L. E., J. N. Connelly, L. E. Nyquist, C.-Y. Shih, H. Wiesmann, and Y. Reese (1999), The age of the carbonates in Martian meteorite ALH84001, *Science*, *286*, 90–94.

Bourke, M. C., and J. J. Wray (2011), Interdune deposits suggest high groundwater in an equatorial crater on Mars, Lunar Planet. Sci., XLII, Abstract 2749.

Boynton, W. V., et al. (2009), Evidence for Calcium Carbonate at the Mars Phoenix Landing Site, *Science*, *325*, 61–64, doi:10.1126/science.1172768.

Bray, V. J., P. M. Schenk, H. J. Melosh, J. V. Morgan, and G. S. Collins (2012), Ganymede crater dimensions—Implications for central peak and central pit formation and development, *Icarus*, *217*, 115–129, doi:10.1016/j.icarus.2011.10.004.

Bridges, J. C., and M. M. Grady (2000), Evaporite mineral assemblages in the nakhlite (Martian) meteorites, *Earth Planet. Sci. Lett.*, *176*, 267–279.

Bridges, J. C., D. C. Catling, J. M. Saxton, T. D. Swindle, I. C. Lyon, and M. M. Grady (2001), Alteration assemblages in Martian meteorites: Implications for near-surface processes, *Space Sci. Rev.*, *96*, 365–392.

Brown, A. J., S. J. Hook, A. M. Baldridge, J. K. Crowley, N. T. Bridges, B. J. Thomson, G. M. Marion, C. R. de Souza Filho, and J. L. Bishop (2010), Hydrothermal formation of clay-carbonate alteration assemblages in the Nili Fossae region of Mars, *Earth Planet. Sci. Lett.*, *297*, 174–182, doi:10.1016/j.epsl.2010.06.018.

Buczkowski, D. L., K. Seelos, S. Murchie, F. Seelos, E. Malaret, C. Hash, and the CRISM Team (2010), Extensive phyllosilicate-bearing layer exposed by valley systems in northwest Noachis Terra, Lunar Planet. Sci., XLI, Abstract 1458.

Buczkowski, D. L., K. Seelos, S. Murchie, F. Seelos, E. Malaret, C. Hash, and the CRISM Team (2013), Evidence for multiple widespread buried phyllosilicate-bearing layers between Argyre and Valles Marineris, Lunar Planet. Sci., XLIV, Abstract 2331.

Bullock, M. A., and J. M. Moore (2007), Atmospheric conditions on early Mars and the missing layered carbonates, *Geophys. Res. Lett.*, *34*, L19201, doi:10.1029/2007GL030688.

Bultel, B., C. Quantin, J. Flahaut, and M. Andréani (2015a), Carbonates and phyllosilicates detections in Coprates Chasma, Valles Marineris, Mars, Lunar Planet. Sci., XLVI, Abstract 2112.

Bultel, B., C. Quantin-Naraf, M. Andréani, H. Clénet, and L. Lozac'h (2015b), Deep alteration between Hellas and Isidis basins, *Icarus*, *260*, 141–160, doi:10.1016/j.icarus.2015.06.037.

Burns, R. G. (1993), Rates and mechanisms of chemical weathering of ferromagnesian silicate minerals on Mars, *Geochim. Cosmochim. Acta*, *57*, 4555–4574.

Calvin, W. M., and J. F. Bell III (2008), Historical context: The pre-MGS view of Mars' surface composition, in *The Martian Surface: Composition, Mineralogy, and Physical Properties*, edited by J. Bell, pp. 20–30, Cambridge Univ. Press, Cambridge.
Calvin, W. M., T. V. V. King, and R. N. Clark (1994), Hydrous carbonates on Mars?: Evidence from Mariner 6/7 infrared spectrometer and ground-based telescopic spectra, *J. Geophys. Res.*, *99*(E7), 14,659–14,675, doi:10.1029/94JE01090.
Cannon, K. M., and J. F. Mustard (2015), Preserved glass-rich impactites on Mars, *Geology*, *43*, 635–638, doi:10.1130/G36953.1.
Cannon, K. M., B. Sutter, D. W. Ming, W. V. Boynton, and R. Quinn (2012), Perchlorate induced low temperature carbonate decomposition in the Mars Phoenix Thermal and Evolved Gas Analyzer (TEGA), *J. Geophys. Res.*, *39*, L13203, doi:10.1029/2012GL051952.
Carr, M. H., and J. W. Head III (2010), Geologic history of Mars, *Earth Planet. Sci. Lett.*, *294*, 185–203, doi:10.1016/j.epsl.2009.06.042.
Carrozzo, F. G., G. Bellucci, F. Altieri, and E. D'Aversa (2013), Detection of carbonate-bearing rocks in craters uplifts of Tyrrhena Terra, Mars, Lunar Planet. Sci., XLIV, Abstract 2241.
Carter, J., and F. Poulet (2012), Orbital identification of clays and carbonates in Gusev crater, *Icarus*, *219*, 250–253, doi:10.1016/j.icarus.2012.02.024.
Carter, J., and F. Poulet (2013), Ancient plutonic processes on Mars inferred from the detection of possible anorthositic terrains, *Nat. Geosci.*, *6*, 1008–1012, doi:10.1038/ngeo1995.
Carter, J., F. Poulet, J.-P. Bibring, and S. Murchie (2010), Detection of hydrated silicates in crustal outcrops in the northern plains of Mars, *Science*, *328*, 1682–1686, doi:10.1126/science.1189013.
Carter, J., F. Poulet, J.-P. Bibring, N. Mangold, and S. Murchie (2013), Hydrous minerals on Mars as seen by the CRISM and OMEGA imaging spectrometers: Updated global view, *J. Geophys. Res. Planets*, *118*, 831–858, doi:10.1029/2012JE004145.
Carter, J., C. Viviano-Beck, D. Loizeau, J. Bishop, and L. Le Deit (2015), Orbital detection and implications of akaganéite on Mars, *Icarus*, *253*, 296–310, doi:10.1016/j.icarus.2015.01.020.
Catling, D. C. (1999), A chemical model for evaporites on early Mars: Possible sedimentary tracers of the early climate and implications for exploration, *J. Geophys. Res.*, *104*(E7), 16,453–16,469, doi:10.1029/1998JE001020.
Changela, H. G., and J. C. Bridges (2011), Alteration assemblages in the nakhlites: Variation with depth on Mars, *Meteorit. Planet. Sci.*, *45*(12), 1847–1867.
Chassefière, E., and F. Leblanc (2011), Methane release and the carbon cycle on Mars, *Planet. Space Sci.*, *59*, 207–217, doi:10.1016/j.pss.2010.09.004.
Chassefière, E., B. Langlais, Y. Quesnel, and F. Leblanc (2013), The fate of early Mars' lost water: The role of serpentinization, *J. Geophys. Res. Planets*, *118*, 1123–1134, doi:10.1002/jgre.20089.
Chevrier, V., F. Poulet, and J.-P. Bibring (2007), Early geochemical environment of Mars as determined from thermodynamics of phyllosilicates, *Nature*, *448*, 60–63, doi:10.1038/nature05961.
Christensen, P. R., et al. (2001), Mars Global Surveyor Thermal Emission Spectrometer experiment: Investigation description and surface science results, *J. Geophys. Res.*, *106*(E10), 23,823–23,871, doi:10.1029/2000JE001370.
Christensen, P. R., et al. (2004), Initial Results from the mini-TES experiment in Gusev Crater from the Spirit Rover, *Science*, *305*, 837–842.
Christensen, P. R., R. L. Fergason, C. S. Edwards, and J. Hill (2013), THEMIS-derived thermal inertia mosaic of Mars: Product description and science results, Lunar Planet. Sci., XLIV, Abstract 2822.
Clark, B. C., S. L. Kenley, D. L. O'Brien, G. R. Huss, R. Mack, and A. K. Baird (1979), Heterogeneous phase reactions of Martian volatiles with putative regolith minerals, *J. Mol. Evol.*, *14*, 91–102.
Clark, R. N., G. A. Swayze, R. Wise, E. Livo, T. Hoefen, R. Kokaly, and S. J. Sutley (2007), USGS digital spectral library splib06a, U.S. Geol. Surv., Digital Data Series 231.
Cloutis, E. A., D. M. Goltz, J. Coombs, B. Russell, M. Guertin, and T. Mueller (2000), Hydrated carbonate minerals: spectral reflectance properties and possibility of detection in Martian spectra, Lunar Planet. Sci., XXXI, Abstract 1152.
Cloutis, E. A., S. E. Grasby, W. M. Last, R. Léveillé, G. R. Osinski, and B. L. Sherriff (2010), Spectral reflectance properties of carbonates from terrestrial analogue environments: Implications for Mars, *Planet. Space Sci.*, *58*, 522–537, doi:10.1016/j.pss.2009.09.002.
Delamere, W. A., et al. (2010), Color imaging of Mars by the High Resolution Imaging Science Experiment (HiRISE), *Icarus*, *205*, 38–52, doi:10.1016/j.icarus.2009.03.012.
Edwards, C. S., and B. L. Ehlmann (2015), Carbon sequestration on Mars, *Geology*, *43*, 863–866, doi:10.1130/G36983.1.
Ehlmann, B. L., and C. S. Edwards (2014), Mineralogy of the Martian surface, *Annu. Rev. Earth Planet. Sci.*, *42*, 291–315, doi:10.1146/annurev-earth-060313-055024.
Ehlmann, B. L., et al. (2008), Orbital identification of carbonate-bearing rocks on Mars, *Science*, *322*, 1828–1832, doi:10.1126/science.1164759.
Ehlmann, B. L., et al. (2009), Identification of hydrated silicate minerals on Mars using MRO-CRISM: Geologic context near Nili Fossae and implications for aqueous alteration, *J. Geophys. Res.*, *114*, E00D08, doi:10.1029/2009JE003339.
Ehlmann, B. L., J. F. Mustard, S. L. Murchie, J.-P. Bibring, A. Meunier, A. A. Fraeman, and Y. Langevin (2011), Subsurface water and clay mineral formation during the early history of Mars, *Nature*, *479*, 53–60, doi:10.1038/nature10582.
Eigenbrode, J. L., H. Bower, and P. Archer Jr. (2014), Decarboxylation of organic compounds as a potential source for CO_2 and CO observed by SAM at Yellowknife Bay, Gale crater, Mars, Lunar Planet. Sci., XLV, Abstract 1605.
Fairén, A. G., D. Fernández-Remolar, J. M. Dohm, V. R. Baker, and R. Amils (2004), Inhibition of carbonate synthesis in acidic oceans on early Mars, *Nature*, *431*, 423–426.
Farquhar, J., and M. H. Thiemens (2000), Oxygen cycle of the Martian atmosphere-regolith system: $\Delta^{17}O$ of secondary phases in Nakhla and Lafayette, *J. Geophys. Res.*, *105*(E5), 11,991–11,997, doi:10.1029/1999JE001194.
Farquhar, J., M. H. Thiemens, and T. Jackson (1998), Atmosphere-surface interactions on Mars: $\Delta^{17}O$ measurements of carbonate from ALH 84001, *Science*, *280*, 1580–1582.
Feely, K. C., and P. R. Christensen (1999), Quantitative compositional analysis using thermal emission spectroscopy: Application to igneous and metamorphic rocks, *J. Geophys. Res.*, *104*(E10), 24,195–24,210, doi:10.1029/1999JE001034.
Fergason, R. L., P. R. Christensen, and H. H. Kieffer (2006), High-resolution thermal inertia derived from the Thermal Emission Imaging System (THEMIS): Thermal model and applications, *J. Geophys. Res.*, *111*, E12004, doi:10.1029/2006JE002735.
Fernández-Remolar, D. C., M. Sánchez-Román, A. C. Hill, D. Gómez-Ortíz, O. P. Ballesteros, C. S. Romanek, and R. Amils (2011), The environment of early Mars and the missing carbonates, *Meteorit. Planet. Sci.*, *46*(10), 1447–1469, doi:10.1111/j.1945-5100.2011.01238.x.
Forget, F., and R. T. Pierrehumbert (1997), Warming early Mars with carbon dioxide clouds that scatter infrared radiation, *Science*, *278*, 1273–1276.
Forget, F., R. Wordsworth, E. Millour, J.-B. Madeleine, L. Kerber, J. Leconte, E. Marcq, and R. M. Haberle (2012), 3D modelling of the early Martian climate under a denser CO_2 atmosphere: Temperatures and CO_2 ice clouds, *Icarus*, *222*, 81–99, doi:10.1016/j.icarus.2012.10.019.

Forsythe, R. D., and J. R. Zimbelman (1995), A case for ancient evaporite basins on Mars, *J. Geophys. Res.*, *100*(E3), 5553–5563, doi:10.1029/95JE00325.
Freissinet, C., et al. (2015), Organic molecules in the Sheepbed Mudstone, Gale Crater, Mars, *J. Geophys. Res. Planets*, *120*, 495–514, doi:10.1002/2014JE004737.
Gaffey, S. J. (1986), Spectral reflectance of carbonate minerals in the visible and near infrared (0.35–2.55 microns): Calcite, aragonite, and dolomite, *Am. Mineral.*, *71*, 151–162.
Gaffey, S. J. (1987), Spectral reflectance of carbonate minerals in the visible and near infrared (0.35–2.55 μm): Anhydrous carbonate minerals, *J. Geophys. Res.*, *92*(B2), 1429–1440, doi:10.1029/JB092iB02p01429.
Garenne, A., G. Montes-Hernandez, P. Beck, B. Schmitt, O. Brissaud, and A. Pommerol (2013), Gas-solid carbonation as a possible source of carbonates in cold planetary environments, *Planet. Space Sci.*, *76*, 28–41, doi:10.1016/j.pss.2012.11.005.
Gilmore, M. S., K. B. Golder, L. Korn, and L. M. Aaron (2014), Carbonate associated with gullies in the Eridania region of Mars, Eighth Int. Conf. on Mars, Abstract 1388.
Glotch, T. D., and A. D. Rogers (2013), Evidence for magma-carbonate interaction beneath Syrtis Major, Mars, *J. Geophys. Res. Planets*, *118*, 126–137, doi:10.1029/2012JE004230.
Goldspiel, J. M., and S. W. Squyres (1991), Ancient aqueous sedimentation on Mars, *Icarus*, *89*, 392–410.
Golombek, M., et al. (2012), Selection of the Mars Science Laboratory landing site, *Space Sci. Rev.*, *170*, 641–737, doi:10.1007/s11214-012-9916-y.
Gooding, J. L., S. J. Wentworth, and M. E. Zolensky (1988), Calcium carbonate and sulfate of possible extraterrestrial origin in the EETA 79001 meteorite, *Geochim. Cosmochim. Acta*, *52*, 909–915.
Goudge, T. A., J. W. Head, J. F. Mustard, and C. I. Fassett (2012), An analysis of open-basin lake deposits on Mars: Evidence for the nature of associated lacustrine deposits and post-lacustrine modification processes, *Icarus*, *219*, 211–229, doi:10.1016/j.icarus.2012.02.027.
Goudge, T. A., K. L. Aureli, J. W. Head, C. I. Fassett, and J. F. Mustard (2015), Classification and analysis of candidate impact crater-hosted closed-basin lakes on Mars, *Icarus*, *260*, 346–367, doi:10.1016/j.icarus.2015.07.026.
Grady, M. M., and I. Wright (2006), The carbon cycle on early Earth—and on Mars?, *Philos. Trans. R. Soc., B*, *361*, 1703–1713, doi:10.1098/rstb.2006.1898.
Grant, J. A., and T. J. Parker (2002), Drainage evolution in the Margaritifer Sinus region, Mars, *J. Geophys. Res.*, *107*(E9), 5066, doi:10.1029/2001JE001678.
Grant, J. A., R. P. Irwin III, J. P. Grotzinger, R. E. Milliken, L. L. Tornabene, A. S. McEwen, C. M. Weitz, S. W. Squyres, T. D. Glotch, and B. J. Thomson (2008), HiRISE imaging of impact megabreccia and sub-meter aqueous strata in Holden Crater, Mars, *Geology*, *36*, 195–198, doi:10.1130/G24340A.1.
Grant, J. A., R. P. Irwin III, and S. A. Wilson (2010), Aqueous depositional settings in Holden crater, Mars, in *Lakes on Mars*, edited by N. Cabrol and E. A. Grin, pp. 323–346, Elsevier, Oxford.
Grant, J. A., M. P. Golombek, J. P. Grotzinger, S. A. Wilson, M. M. Watkins, A. R. Vasavada, J. L. Griffes, and T. J. Parker (2011), The science process for selecting the landing site for the 2011 Mars Science Laboratory, *Planet. Space Sci.*, *59*, 1114–1127, doi:10.1016/j.pss.2010.06.016.
Grotzinger, J. P., and R. E. Milliken (2012), The sedimentary rock record of Mars: Distribution, origins, and global stratigraphy, in *Sedimentary Geology of Mars*, *Spec. Publ.*, vol. 102, edited by J. P. Grotzinger and R. E. Milliken, pp. 1–48, SEPM Soc. for Sediment. Geol., Tulsa, Okla.
Grotzinger, J. P., et al. (2015), Deposition, exhumation, and paleoclimate of an ancient lake deposit, Gale crater, Mars, *Science*, *350*(6257), aac7575, doi:10.1126/science.aac7575.
Hagerty, J. J., and H. E. Newsom (2003), Hydrothermal alteration at the Lonar Lake impact structure, India: Implications for impact cratering on Mars, *Meteorit. Planet. Sci.*, *38*(3), 365–381.
Halevy, I., W. W. Fischer, and J. M. Eiler (2011), Carbonates in the Martian meteorite Allan Hills 84001 formed at 18 ± 4°C in a near-surface aqueous environment, *Proc. Natl. Acad. Sci. U.S.A.*, *108*, 16,895–16,899, doi:10.1073/pnas.1109444108.
Hardie, L. A., and H. P. Eugster (1970), The evolution of closed-basin brines, *Mineral. Soc. Am. Spec. Pap.*, *3*, 273–290.
Harner, P. L., and M. S. Gilmore (2015), Visible–near infrared spectra of hydrous carbonates, with implications for the detection of carbonates in hyperspectral data of Mars, *Icarus*, *250*, 204–214, doi:10.1016/j.icarus.2014.11.037.
Harvey, R. P., and H. Y. McSween Jr. (1996), A possible high-temperature origin for the carbonates in the Martian meteorite ALH84001, *Nature*, *382*, 49–51.
Hecht, M. H. (2002), Metastability of liquid water on Mars, *Icarus*, *156*, 373–386, doi:10.1006/icar.2001.6794.
Horgan, B., and J. F. Bell III (2012), Widespread weathered glass on the surface of Mars, *Geology*, *40*, 391–394, doi:10.1130/G32755.1.
Hörz, F., P. D. Archer Jr., P. B. Niles, M. E. Zolensky, and M. Evans (2015), Devolatilization or melting of carbonates at Meteor Crater, AZ?, *Meteorit. Planet. Sci.*, *50*, 1050–1070, doi:10.1111/maps.12453.
Hu, R., D. M. Kass, B. L. Ehlmann, and Y. L. Yung (2015), Tracing the fate of carbon and the atmospheric evolution of Mars, *Nat. Commun.*, *6*, 10003, doi:10.1038/ncomms10003.
Huang, C. K., and P. F. Kerr (1960), Infrared study of the carbonate minerals, *Am. Mineral.*, *45*, 311–324.
Hunt, G. R., and J. W. Salisbury (1971), Visible and near-infrared spectra of minerals and rocks: II. Carbonates, *Mod. Geol.*, *2*, 23–30.
Hurowitz, J. A., W. W. Fischer, N. J. Tosca, and R. E. Milliken (2010), Origin of acidic surface waters and the evolution of atmospheric chemistry on early Mars, *Nat. Geosci.*, *3*, 323–326, doi:10.1038/ngeo831.
Ingersoll, A. P. (1970), Mars: Occurrence of liquid water, *Science*, *168*, 972–973.
Irwin, R. P., III, J. J. Wray, T. A. Maxwell, S. C. Mest, and S. T. Hansen (2012), Wind-eroded stratigraphy on the floor of a Noachian impact crater, Noachis Terra, Mars, Third Int. Conf. on Early Mars, Abstract 7066.
Jain, N., and P. Chauhan (2015), Study of phyllosilicates and carbonates from the Capri Chasma region of Valles Marineris on Mars based on Mars Reconnaissance Orbiter-Compact Reconnaissance Imaging Spectrometer for Mars (MRO-CRISM) observations, *Icarus*, *250*, 7–17, doi:10.1016/j.icarus2014.11.018.
Jakosky, B. M., and J. H. Jones (1997), The history of Martian volatiles, *Rev. Geophys.*, *35*, 1–16.
Jakosky, B. M., and R. J. Phillips (2001), Mars' volatile and climate history, *Nature*, *412*, 237–244.
Jouglet, D., F. Poulet, J. P. Bibring, Y. Langevin, and B. Gondet (2007), Search for carbonates on Mars with the OMEGA / Mars Express data, Lunar Planet. Inst. Contrib., 1353, Abstract 3153.
Kahn, R. (1985), The Evolution of CO_2 on Mars, *Icarus*, *62*, 175–190.
Karunatillake, S., et al. (2006), Composition of northern low-albedo regions of Mars: Insights from the Mars Odyssey Gamma Ray Spectrometer, *J. Geophys. Res.*, *111*, E03S05, doi:10.1029/2006JE002675.
Karunatillake, S., J. J. Wray, S. W. Squyres, G. J. Taylor, O. Gasnault, S. M. McLennan, W. Boynton, M. R. El Maarry, and J. M. Dohm (2009), Chemically striking regions on Mars and Stealth revisited, *J. Geophys. Res.*, *114*, E12001, doi:10.1029/2008JE003303.

Karunatillake, S., J. J. Wray, O. Gasnault, S. M. McLennan, A. D. Rogers, S. W. Squyres, W. V. Boynton, J. R. Skok, L. Ojha, and N. Olsen (2014), Sulfates hydrating bulk soil in the Martian low and middle latitudes, *Geophys. Res. Lett.*, *41*, 7987–7996, doi:10.1002/2014GL061136.
Kasting, J. F. (1991), CO_2 condensation and the climate of early Mars, *Icarus*, *94*, 1–13.
Kirkland, L. E., K. C. Herr, and P. M. Adams (2003), Infrared stealthy surfaces: Why TES and THEMIS may miss some substantial mineral deposits on Mars and implications for remote sensing of planetary surfaces, *J. Geophys. Res.*, *108*(E12), 5137, doi:10.1029/2003JE002105.
Kite, E. S., J.-P. Williams, A. Lucas, and O. Aharonson (2014), Low palaeopressure of the Martian atmosphere estimated from the size distribution of ancient craters, *Nat. Geosci.*, *7*, 335–339, doi:10.1038/ngeo2137.
Korn, L. K., and M. S. Gilmore (2015), Possible carbonate minerals within an unnamed gullied crater in Eridania basin, Mars, Lunar Planet. Sci., XLVI, Abstract 2224.
Kounaves, S. P., et al. (2010a), Wet Chemistry experiments on the 2007 Phoenix Mars Scout Lander mission: Data analysis and results, *J. Geophys. Res. Lett.*, *115*, E00E10, doi:10.1029/2009JE003424.
Kounaves, S. P., et al. (2010b), Soluble sulfate in the Martian soil at the Phoenix landing site, *Geophys. Res. Lett.*, *37*, L09201, doi:10.1029/2010GL042613.
Kral, T. A., W. Birch, L. E. Lavender, and B. T. Virden (2014), Potential use of highly insoluble carbonates as carbon sources by methanogens in the subsurface of Mars, *Planet. Space Sci.*, *101*, 181–185, doi:10.1016/j.pss.2014.07.008.
Lammer, H., et al. (2013), Outgassing history and escape of the Martian atmosphere and water inventory, *Space Sci. Rev.*, *174*, 113–154, doi:10.1007/s11214-012-9943-8.
Lapen, T. J., M. Righter, A. D. Brandon, V. Debaille, B. L. Beard, J. T. Shafer, and A. H. Peslier (2010), A younger age for ALH84001 and its geochemical link to shergottite sources in Mars, *Science*, *328*, 347–351, doi:10.1126/science.1185395.
Le Deit, L., J. Flahaut, C. Quantin, E. Hauber, D. Mège, O. Bourgeois, J. Gurgurewicz, M. Massé, and R. Jaumann (2012), Extensive surface pedogenic alteration of the Martian Noachian crust suggested by plateau phyllosilicates around Valles Marineris, *J. Geophys. Res.*, *117*, E00J05, doi:10.1029/2011JE003983.
Lellouch, E., T. Encrenaz, T. de Graauw, S. Erard, P. Morris, J. Crovisier, H. Feuchtgruber, T. Girard, and M. Burgdorf (2000), The 2.4–45 μm spectrum of Mars observed with the Infrared Space Observatory, *Planet. Space Sci.*, *48*, 1393–1405.
Leshin, L. A., et al. (2013), Volatile, isotope, and organic analysis of Martian fines with the Curiosity rover, *Science*, *341*, 1238937, doi:10.1126/science.1238937.
Manga, M., A. Patel, J. Dufek, and E. S. Kite (2012), Wet surface and dense atmosphere on early Mars suggested by the bomb sag at Home Plate, Mars, *Geophys. Res. Lett.*, *39*, L01202, doi:10.1029/2011GL050192.
McEwen, A. S., L. Tornabene, J. Grant, J. Wray, and J. Mustard (2008), Noachian Megabreccia on Mars, Eos Trans. AGU, 89(53), Fall Meet. Suppl., Abstract P43D-03.
McGuire, P. C., et al. (2009), An improvement to the volcano-scan algorithm for atmospheric correction of CRISM and OMEGA spectral data, *Planet. Space Sci.*, *57*, 809–815, doi:10.1016/j.pss.2009.03.007.
McKay, C. P., and S. S. Nedell (1988), Are there carbonate deposits in the Valles Marineris, Mars?, *Icarus*, *73*, 142–148.
Michalski, J. R., and P. B. Niles (2010), Deep crustal carbonate rocks exposed by meteor impact on Mars, *Nat. Geosci.*, *3*, 751–755, doi:10.1038/ngeo971.
Michalski, J. R., J. Cuadros, P. B. Niles, J. Parnell, A. D. Rogers, and S. P. Wright (2013), Groundwater activity on Mars and implications for a deep biosphere, *Nat. Geosci.*, *6*, 133–138, doi:10.1038/ngeo1706.
Milliken, R. E., and D. L. Bish (2010), Sources and sinks of clay minerals on Mars, *Philos. Mag.*, *90*, 2293–2308, doi:10.1080/14786430903575132.
Milliken, R. E., T. Bristow, and D. L. Bish (2011), Diagenesis of clay minerals on Mars and implications for the Mars Science Laboratory rover, Lunar Planet. Sci., XLII, Abstract 2230.
Ming, D. W., et al. (2014), Volatile and organic compositions of sedimentary rocks in Yellowknife Bay, Gale Crater, Mars, *Science*, *343*(6169), 1245267, doi:10.1126/science.1245267.
Mittlefehldt, D. W. (1994), ALH84001, a cumulate orthopyroxenite member of the Martian meteorite clan, *Meteoritics*, *29*, 214–221.
Miyamoto, M., and A. Kato (1990), Infrared diffuse reflectance spectra of some hydrous carbonates, Lunar Planet. Sci., XXI, 801–802.
Morris, R. V., D. W. Ming, D. C. Golden, T. G. Graff, and C. N. Achilles (2010a), Evidence for interlayer collapse of nontronite on Mars from laboratory visible and near-IR reflectance spectra, Lunar Planet. Sci., XLI, Abstract 2156.
Morris, R. V., et al. (2010b), Identification of carbonate-rich outcrops on Mars by the Spirit Rover, *Science*, *329*, 421–424, doi:10.1126/science.1189667.
Murchie, S., L. Kirkland, S. Erard, J. Mustard, and M. Robinson (2000), Near-infrared spectral variations of Martian surface materials from ISM imaging spectrometer data, *Icarus*, *147*, 444–471.
Murchie, S., et al. (2007), Compact Reconnaissance Imaging Spectrometer for Mars (CRISM) on Mars Reconnaissance Orbiter (MRO), *J. Geophys. Res.*, *112*, E05S03, doi:10.1029/2006JE002682.
Murchie, S. L., et al. (2009a), A synthesis of Martian aqueous mineralogy after 1 Mars year of observations from the Mars Reconnaissance Orbiter, *J. Geophys. Res.*, *114*, E00D06, doi:10.1029/2009JE003342.
Murchie, S. L., et al. (2009b), Compact Reconnaissance Imaging Spectrometer for Mars investigation and data set from the Mars Reconnaissance Orbiter's primary science phase, *J. Geophys. Res.*, *114*, E00D07, doi:10.1029/2009JE003344.
Mustard, J. F., F. Poulet, A. Gendrin, J.-P. Bibring, Y. Langevin, B. Gondet, N. Mangold, G. Bellucci, and F. Altieri (2005), Olivine and pyroxene diversity in the crust of Mars, *Science*, *307*, 1594–1597, doi:10.1126/science.1109098.
Mustard, J. F., F. Poulet, J. W. Head, N. Mangold, J.-P. Bibring, S. M. Pelkey, C. I. Fassett, Y. Langevin, and G. Neukum (2007), Mineralogy of the Nili Fossae region with OMEGA/Mars Express data: 1. Ancient impact melt in the Isidis Basin and implications for the transition from the Noachian to Hesperian, *J. Geophys. Res.*, *112*, E08S03, doi:10.1029/2006JE002834.
Mustard, J. F., et al. (2008), Hydrated silicate minerals on Mars observed by the Mars Reconnaissance Orbiter CRISM instrument, *Nature*, *454*, 305–309, doi:10.1038/nature07097.
Niles, P. B., and J. Michalski (2009), Meridiani Planum sediments on Mars formed through weathering in massive ice deposits, *Nat. Geosci.*, *2*, 215–220, doi:10.1038/ngeo438.
Niles, P. B., W. V. Boynton, J. H. Hoffman, D. W. Ming, and D. Hamara (2010), Stable isotope measurements of Martian atmospheric CO_2 at the Phoenix landing site, *Science*, *329*, 1334–1337, doi:10.1126/science.1192863.
Niles, P. B., D. C. Catling, G. Berger, E. Chassefière, B. L. Ehlmann, J. R. Michalski, R. Morris, S. W. Ruff, and B. Sutter (2013), Geochemistry of carbonates on Mars: Implications for climate history and nature of aqueous environments, *Space Sci. Rev.*, *174*, 301–328.
Niles, P. B., et al. (2015), Investigating CO_2 reservoirs at Gale crater and evidence for a dense early atmosphere, Lunar Planet. Sci., XLVI, Abstract 2840.

O'Connor, J. T. (1968), "Fossil" Martian weathering, *Icarus*, *8*, 513–517.
Orofino, V., J. Goldspiel, I. Carofalo, A. Blanco, S. Fonti, and G. A. Marzo (2009), Evaluation of carbonate abundance in putative Martian paleolake basins, *Icarus*, *200*, 426–435, doi:10.1016/j.icarus.2008.11.020.
Osinski, G. R. (2003), Impact glasses in fallout suevites from the Ries impact structure, Germany: An analytical SEM study, *Meteorit. Planet. Sci.*, *38*(11), 1641–1667.
Osinski, G. R., J. G. Spray, and P. Lee (2001), Impact-induced hydrothermal activity within the Haughton impact structure, arctic Canada: Generation of a transient, warm, wet oasis, *Meteorit. Planet. Sci.*, *36*, 731–745.
Osinski, G. R., R. A. F. Grieve, and J. G. Spray (2004), The nature of the groundmass of surficial suevite from the Ries impact structure, Germany, and constraints on its origin, *Meteorit. Planet. Sci.*, *39*(10), 1655–1683.
Osinski, G. R., P. Lee, J. Parnell, J. G. Spray, and M. Baron (2005), A case study of impact-induced hydrothermal activity: The Haughton impact structure, Devon Island, Canadian High Arctic, *Meteorit. Planet. Sci.*, *40*(12), 1859–1877.
Palomba, E., A. Zinzi, E. A. Cloutis, M. D'Amore, D. Grassi, and A. Maturilli (2009), Evidence for Mg-rich carbonates on Mars from a 3.9 μm absorption feature, *Icarus*, *203*, 58–65, doi:10.1016/j.icarus.2009.04.013.
Peel, S. E., and C. I. Fassett (2013), Valleys in pit craters on Mars: Characteristics, distribution, and formation mechanisms, *Icarus*, *225*, 272–282, doi:10.1016/j.icarus.2013.03.031.
Pelkey, S. M., et al. (2007), CRISM multispectral summary products: Parameterizing mineral diversity on Mars from reflectance, *J. Geophys. Res.*, *112*, E08S14, doi:10.1029/2006JE002831.
Pentecost, A. (1995), Geochemistry of carbon dioxide in six travertine-depositing waters of Italy, *J. Hydrol.*, *167*, 263–278.
Phillips, R. J., et al. (2011), Massive CO_2 ice deposits sequestered in the south polar layered deposits of Mars, *Science*, *332*, 838–841, doi:10.1126/science.1203091.
Pollack, J. B., J. F. Kasting, S. M. Richardson, and K. Poliakoff (1987), The case for a warm, wet climate on early Mars, *Icarus*, *71*, 203–224.
Pollack, J. B., T. Roush, F. Witteborn, J. Bregman, D. Wooden, C. Stoker, O. B. Toon, D. Rank, B. Dalton, and R. Freedman (1990), Thermal Emission Spectra of Mars (5.4–10.5 μm): Evidence for sulfates, carbonates, and hydrates, *J. Geophys. Res.*, *95*(B9), 14,595–14,627, doi:10.1029/JB095iB09p14595.
Poulet, F., J.-P. Bibring, J. F. Mustard, A. Gendrin, N. Mangold, Y. Langevin, R. E. Arvidson, B. Gondet, C. Gomez, and the Omega Team (2005), Phyllosilicates on Mars and Implications for early Martian climate, *Nature*, *438*, 623–627, doi:10.1038/nature04274.
Poulet, F., J. Carter, J. L. Bishop, D. Loizeau, and S. M. Murchie (2014), Mineral abundances at the final four Curiosity study sites and implications for their formation, *Icarus*, *231*, 65–76, doi:10.1016/j.icarus.2013.11.023.
Putzig, N. E., and M. T. Mellon (2007), Apparent thermal inertia and the surface heterogeneity of Mars, *Icarus*, *191*, 68–94, doi:10.1016/j.icarus.2007.05.013.
Ramirez, R. M., R. Kopparapu, M. E. Zugger, T. D. Robinson, R. Freedman, and J. F. Kasting (2014), Warming early Mars with CO_2 and H_2, *Nat. Geosci.*, *7*, 59–63, doi:10.1038/ngeo2000.
Ramsey, M. S., and P. R. Christensen (1998), Mineral abundance determination: Quantitative deconvolution of thermal emission spectra, *J. Geophys. Res.*, *103*(B1), 577–596, doi:10.1029/97JB02784.
Richardson, M. I., and M. A. Mischna (2005), Long-term evolution of transient liquid water on Mars, *J. Geophys. Res.*, *110*, E03003, doi:10.1029/2004JE002367.
Romanek, C. S., C. Jiménez-López, A. Rodriguez Navarro, M. Sánchez-Román, N. Sahai, and M. Coleman (2009), Inorganic synthesis of Fe-Ca-Mg carbonates at low temperature, *Geochim. Cosmochim. Acta*, *73*, 5361–5376, doi:10.1016/j.gca.2009.05.065.
Rosing, M. T. (1999), ^{13}C-Depleted carbon microparticles in >3700-Ma sea-floor sedimentary rocks from West Greenland, *Science*, *283*, 674–676.
Ruff, S. W., P. R. Christensen, R. N. Clark, H. H. Kieffer, M. C. Malin, J. L. Bandfield, B. M. Jakosky, M. D. Lane, M. T. Mellon, and M. A. Presley (2001), Mars' "White Rock" feature lacks evidence of an aqueous origin: Results from Mars Global Surveyor, *J. Geophys. Res.*, *106*(E10), 23,921–23,927, doi:10.1029/2000JE001329.
Ruff, S. W., P. B. Niles, F. Alfano, and A. B. Clarke (2014), Evidence for a Noachian-aged ephemeral lake in Gusev crater, Mars, *Geology*, *42*, 359–362, doi:10.1130/G35508.1.
Seelos, F. P., S. L. Murchie, D. C. Humm, O. S. Barnouin, F. Morgan, H. W. Taylor, C. Hash, and The CRISM Team (2011), CRISM data processing and analysis products update—Calibration, correction, and visualization, Lunar Planet. Sci., XLII, Abstract 1438.
Seelos, F. P., M. F. Morgan, H. W. Taylor, S. L. Murchie, D. C. Humm, K. D. Seelos, O. S. Barnouin, C. E. Viviano, and the CRISM Team (2012), CRISM Map projected Targeted Reduced Data Records (MTRDRs)—High level analysis and visualization data products, in *Planetary Data: A Workshop for Users and Software Developers*, edited by L. R. Gaddis et al., pp. 159–162, U.S. Geol. Surv., Flagstaff, Ariz.
Seelos, K. D., O. S. Barnouin, and the CRISM Team (2010), Huygens crater and the highland terrains in western Tyrrhena Terra: Mineralogic mapping with CRISM data, Lunar Planet. Sci., XLI, Abstract 2400.
Shaheen, R., A. Abramian, J. Horn, G. Dominguez, R. Sullivan, and M. H. Thiemens (2010), Detection of oxygen isotopic anomaly in terrestrial atmospheric carbonates and its implications to Mars, *Proc. Natl. Acad. Sci. U.S.A.*, *107*, 20,213–20,218, doi:10.1073/pnas.1014399107.
Shaheen, R., P. B. Niles, K. Chong, C. M. Corrigan, and M. H. Thiemens (2015), Carbonate formation events in ALH 84001 trace the evolution of the Martian atmosphere, *Proc. Natl. Acad. Sci. U.S.A.*, *112*, 336–341, doi:10.1073/pnas.1315615112.
Smith, D. E., et al. (1999), The global topography of Mars and implications for surface evolution, *Science*, *284*, 1495–1503, doi:10.1126/science.284.5419.1495.
Smyth, S., D. M. Applin, M. R. M. Izawa, and E. A. Cloutis (2014), Diffuse reflectance spectra of monohydrocalcite, Lunar Planet. Sci., XLV, Abstract 2899.
Squyres, S. W., et al. (2004), The Spirit Rover's Athena science investigation at Gusev Crater, Mars, *Science*, *305*, 794–799, doi:10.1126/science.3050794.
Stephens, S. K., and D. J. Stevenson (1990), Dry carbonate formation on Mars: A plausible sink for an early dense CO_2 atmosphere?, Lunar Planet. Sci., XXI, 1198–1199.
Stephens, S. K., D. J. Stevenson, and G. R. Rossman (1995), Carbonates on Mars: Experimental results, Lunar Planet. Sci., XXVI, 1355–1356.
Stockstill, K. R., J. E. Moersch, S. W. Ruff, A. Baldridge, and J. Farmer (2005), Thermal Emission Spectrometer hyperspectral analyses of proposed paleolake basins on Mars: No evidence for in-place carbonates, *J. Geophys. Res.*, *110*, E10004, doi:10.1029/2004JE002353.
Stockstill, K. R., J. E. Moersch, H. Y. McSween Jr., J. Piatek, and P. R. Christensen (2007), TES and THEMIS study of proposed paleolake basins within the Aeolis quadrangle of Mars, *J. Geophys. Res.*, *112*, E01001, doi:10.1029/2005JE002517.
Summons, R. E., J. P. Amend, D. Bish, R. Buick, G. D. Cody, D. J. Des Marais, G. Dromart, J. L. Eigenbrode, A. H. Knoll, and D. Y. Sumner (2011), Preservation of Martian organic and environmental records: Final report of the Mars Biosignature Working Group, *Astrobiology*, *11*, 157–181.

Sun, V. Z., and R. E. Milliken (2014), The geology and mineralogy of Ritchey crater, Mars: Evidence for post-Noachian clay formation, *J. Geophys. Res. Planets*, *119*, 810–836, doi:10.1002/2013JE004602.

Sutter, B., W. V. Boynton, D. W. Ming, P. B. Niles, R. V. Morris, D. C. Golden, H. V. Lauer, C. Fellows, D. K. Hamara, and S. A. Mertzman (2012), The detection of carbonate in the Martian soil at the Phoenix landing site: A laboratory investigation and comparison with Thermal and Evolved Gas Analyzer (TEGA) data, *Icarus*, *218*, 290–296, doi:10.1016/j.icarus.2011.12.002.

Toon, O. B., J. B. Pollack, W. Ward, J. A. Burns, and K. Bilski (1980), The astronomical theory of climatic change on Mars, *Icarus*, *44*, 552–607.

Tornabene, L. L., J. E. Moersch, H. Y. McSween Jr., V. E. Hamilton, J. L. Piatek, and P. R. Christensen (2008), Surface and crater-exposed lithologic units of the Isidis Basin as mapped by coanalysis of THEMIS and TES derived data products, *J. Geophys. Res.*, *113*, E10001, doi:10.1029/2007JE002988.

Tornabene, L. L., G. R. Osinski, A. S. McEwen, J. M. Boyce, V. J. Bray, C. M. Caudill, J. A. Grant, C. W. Hamilton, S. Mattson, and P. J. Mouginis-Mark (2012), Widespread crater-related pitted materials on Mars: Further evidence for the role of target volatiles during the impact process, *Icarus*, *220*, 348–368, doi:10.1016/j.icarus.2012.05.022.

Tosca, N. J., and S. M. McLennan (2006), Chemical divides and evaporite assemblages on Mars, *Earth Planet. Sci. Lett.*, *241*, 21–31, doi:10.1016/j.epsl.2005.10.021.

Urata, R. A., and O. B. Toon (2013), Simulations of the Martian hydrologic cycle with a general circulation model: Implications for the ancient Martian climate, *Icarus*, *226*, 229–250, doi:10.1016/j.icarus.2013.05.014.

Valley, J. W., J. M. Eiler, C. M. Graham, E. K. Gibson, C. S. Romanek, and E. M. Stolper (1997), Low-temperature carbonate concretions in the Martian meteorite ALH84001: Evidence from stable isotopes and mineralogy, *Science*, *275*, 1633–1638.

Van Berk, W., and Y. Fu (2011), Reproducing hydrogeochemical conditions triggering the formation of carbonate and phyllosilicate alteration mineral assemblages on Mars (Nili Fossae region), *J. Geophys. Res.*, *116*, E10006, doi:10.1029/2011JE003886.

Van Berk, W., J.-M. Ilger, Y. Fu, and C. Hansen (2011), Decreasing CO_2 partial pressure triggered Mg-Fe-Ca carbonate formation in ancient Martian crust preserved in the ALH84001 meteorite, *Geofluids*, *11*, 6–17, doi:10.1111/j.1468-8123.2010.00296.x.

Van Berk, W., Y. Fu, and J.-M. Ilger (2012), Reproducing early Martian atmospheric carbon dioxide partial pressure by modeling the formation of Mg-Fe-Ca carbonate identified in the Comanche rock outcrops on Mars, *J. Geophys. Res.*, *117*, E10008, doi:10.1029/2012JE004173.

Vaniman, D. T., D. L. Bish, and S. J. Chipera (2008), Calcium sulfate hydration, stability, and transformation on Mars, Lunar Planet. Sci., XXXIX, Abstract 1816.

Viviano-Beck, C. E. (2015), Early hydrothermal environments on Mars: Tyrrhena Terra, Lunar Planet. Sci., XLVI, Abstract 2756.

Viviano-Beck, C. E., and S. L. Murchie (2014), Phyllosilicates in the walls of Valles Marineris and the tectonic evolution of the greater Tharsis region, Eighth Int. Conf. on Mars, Abstract 1220.

Viviano-Beck, C. E., et al. (2014), Revised CRISM spectral parameters and summary products based on the currently detected mineral diversity on Mars, *J. Geophys. Res. Planets*, *119*, 1403–1431, doi:10.1002/2014JE004627.

Warren, P. H. (1987), Mars regolith versus SNC meteorites: Possible evidence for abundant crustal carbonates, *Icarus*, *70*, 153–161.

Webster, C. R., and P. R. Mahaffy (2011), Determining the local abundance of Martian methane and its $^{13}C/^{12}C$ and D/H isotopic ratios for comparison with related gas and soil analysis on the 2011 Mars Science Laboratory (MSL) mission, *Planet. Space Sci.*, *59*, 271–283, doi:10.1016/j.pss.2010.08.021.

Wentworth, S. J., and J. L. Gooding (1994), Carbonates and sulfates in the Chassigny meteorite: Further evidence for aqueous chemistry on the SNC parent planet, *Meteoritics*, *29*, 860–863.

Werner, S. C. (2008), The early Martian evolution—Constraints from basin formation ages, *Icarus*, *195*, 45–60, doi:10.1016/j.icarus.2007.12.008.

Werner, S. C., and K. L. Tanaka (2011), Redefinition of the crater-density and absolute-age boundaries for the chronostratigraphic system of Mars, *Icarus*, *215*, 603–607, doi:10.1016/j.icarus.2011.07.024.

Williams, N. R., J. F. Bell III, P. R. Christensen, and J. D. Farmer (2015), Evidence for an explosive origin of central pit craters on Mars, *Icarus*, *252*, 175–185, doi:10.1016/j.icarus.2014.12.005.

Wiseman, S. M., B. L. Ehlmann, and J. F. Mustard (2014), Characterization of carbonate compositions and mineral assemblages to constrain geochemical conditions, Lunar Planet. Sci., XLV, Abstract 2249.

Wray, J. J., S. L. Murchie, S. W. Squyres, F. P. Seelos, and L. L. Tornabene (2009), Diverse aqueous environments on ancient Mars revealed in the southern highlands, *Geology*, *37*, 1043–1046, doi:10.1130/G30331A.1.

Wray, J. J., S. W. Squyres, L. H. Roach, J. L. Bishop, J. F. Mustard, and E. Z. Noe Dobrea (2010), Identification of the Ca-sulfate bassanite in Mawrth Vallis, Mars, *Icarus*, *209*, 416–421, doi:10.1016/j.icarus.2010.06.001.

Wray, J. J., S. T. Hansen, J. Dufek, G. A. Swayze, S. L. Murchie, F. P. Seelos, J. R. Skok, R. P. Irwin III, and M. S. Ghiorso (2013), Prolonged magmatic activity on Mars inferred from the detection of felsic rocks, *Nat. Geosci.*, *6*, 1013–1017, doi:10.1038/ngeo1994.

Zent, A. P., and R. C. Quinn (1995), Simultaneous adsorption of CO_2 and H_2O under Mars-like conditions and application to the evolution of the Martian climate, *J. Geophys. Res.*, *100*(E3), 5341–5349, doi:10.1029/94JE01899.

Zolotov, M. Y., and E. L. Shock (2005), Formation of jarosite-bearing deposits through aqueous oxidation of pyrite at Meridiani Planum, Mars, *Geophys. Res. Lett.*, *32*, L21203, doi:10.1029/2005GL024253.